Mineral Spectroscopy: A Tribute to Roger G. Burns
© The Geochemical Society, Special Publication No. 5, 1996
Editors: M. D. Dyar, C. McCammon and M. W. Schaefer

Schwertmannite on Mars? Spectroscopic analyses of schwertmannite, its relationship to other ferric minerals, and its possible presence in the surface material on Mars.

JANICE L. BISHOP[1] and ENVER MURAD[2]

[1]DLR, Institute for Planetary Exploration, Rudower Chaussee 5, D-12489 Berlin, Germany
[2]Bayerisches Geologisches Landesamt, D-96033 Bamberg, Germany

Abstract—Schwertmannite, a hydroxylated ferric sulfate mineral, is presented as a possible component of the surface material on Mars. Schwertmannite could have formed on Mars through chemical weathering processes as acidic groundwater came in contact with the atmosphere. Visible and infrared reflectance spectra of schwertmannite are presented here and analyzed in the context of spectra of other ferric minerals and Mars soil analogs. Infrared transmittance spectra and Mössbauer spectra of schwertmannite are studied as well to facilitate interpretation of the reflectance spectra. The visible region spectra of schwertmannite are similar to those of jarosite and akaganéite in that they are dominated by a broad Fe^{3+} transition near 0.91 μm and a local reflectance maximum near 0.73 μm. Spectra of schwertmannite are relatively bright in the near infrared and exhibit broad bound and adsorbed water features near 1.45, 1.95 and 3 μm. The mid-infrared region spectra are significantly darker and include a water feature near 6.1 μm and several weak sulfate and OH features at longer wavelengths. The formation conditions and spectral features of schwertmannite are consistent with those of the ferric sulfate phase present in chemically-treated ferric sulfate-bearing montmorillonites, which have been examined as Mars soil analogs. Methods suitable for detecting the possible presence of schwertmannite in the martian surface soil are discussed, as well as implications for the surface geochemistry of Mars should schwertmannite occur there.

INTRODUCTION

Ferric sulfates and gossans have been proposed as components of the martian surface material due to their occurrence on Earth as weathering products under aqueous conditions that could have arisen on Mars under an earlier warm, wet climate (BURNS, 1987; BURNS, 1988). More recently BURNS (1994) suggested the formation of the hydroxylated ferric sulfate mineral schwertmannite in equatorial regions of Mars, where acidic permafrost melts and is oxidized by the martian atmosphere. Schwertmannite is often associated with ferrihydrite (BIGHAM *et al.*, 1992; SCHWERTMANN *et al.*, 1995), a ferric oxyhydroxide that has been proposed as a component of the soil on Mars (BISHOP *et al.*, 1993; BISHOP and PIETERS, 1995). BURNS (1994) described schwertmannite formation under conditions of laterization and ferric oxide deposition in a warm and humid environment depleted in dissolved K and Al, followed by a period of aridity. This pattern has been observed in regions of Australia and was proposed by BURNS (1994) for the equatorial regions on Mars. It is consistent with the development of groundwater under ancient martian climatic conditions, from martian crustal materials thought to be low in K and Al.

Many areas in the martian bright regions, such as the Tharsis and Amazonis plateau plains, exhibit weak visible ferric absorption features consistent with those of hematite (*e.g.*, MCCORD *et al.*, 1982; BELL *et al.*, 1990; MURCHIE *et al.*, 1993). Spectral analyses of hematites with variable particle sizes indicate that Mars-like spectral signatures can be achieved from combinations of crystalline and nanophase hematite, but neither alone (MORRIS *et al.*, 1989). Initial spectral mixing experiments indicate that a maximum of 1 wt.% bulk, crystalline hematite should be present in the martian soil in order to give the observed spectral properties for many martian bright regions (SINGER, 1982). Additional mixing experiments by MORRIS *et al.* (1989) and MORRIS and LAUER (1990) using fine-grained (''type S + D'', approximately <2.0 μm particle size) hematite that exhibits characteristic bulk hematite extended visible region spectral features, showed that mixtures containing ~1, ~3, and ~5 wt.% Fe_2O_3 of this fine-grained, crystalline hematite produced a spectrum in the extended visible region consistent with a Mars bright region spectrum (SINGER *et al.*, 1979).

There is ~18–20 wt.% Fe_2O_3 present in the martian soils measured by Viking (TOULMIN *et al.*, 1977). Based on the work of SINGER (1982) and MORRIS *et al.* (1989), ~1–5 wt.% Fe_2O_3 in the martian bright region soil can be ''crystalline'' hematite, i.e. hematite exhibiting the spectral properties characteristic of bulk hematite. The remaining ~13–19 wt.% Fe_2O_3 in the martian surface mate-

rial is not present as "crystalline" hematite and is probably present as (i) one or more nanophase ferric minerals, (ii) incorporated into the silicate matrix material (*e.g.,* spectrally neutral basalt or smectites, where some of the structural cation sites are filled by Fe) and/or (iii) amorphous ferric species. Nanophase hematite grown in silica gel (MORRIS *et al.,* 1989; MORRIS and LAUER, 1990), nanophase hematite found in palagonitic soils (MORRIS *et al.,* 1990, 1993; GOLDEN *et al.,* 1993), ferrihydrite (BISHOP *et al.,* 1993), and nanophase ferric oxides/oxyhydroxides/oxyhydroxysulfates grown in chemically-treated montmorillonites (BANIN *et al.,* 1993; BISHOP *et al.,* 1993, 1995) have been studied as potential candidates for this nanophase component of the ferric iron in Mars surface material.

In addition to the bright region Mars soils having a weak visible feature near 0.86 μm, which is consistent with hematite, the less common bright region Mars soils having weak visible features at longer wavelengths must be considered. Lunae Planum and the Oxia region of western Arabia exhibit ferric absorption features near 0.88 and 0.92 μm, respectively (MCCORD *et al.,* 1977, 1982; MURCHIE *et al.,* 1993; S. MURCHIE, pers. comm., 1995). These absorptions are not consistent with the component of bulk hematite inferred to be present in the more common bright regions, such as Tharsis and Amazonis, and may indicate a different crystalline ferric phase. However, nanophase and nonpigmentary components of the surface material in these uncommon regions might still be similar to those in the regions where an 0.86 μm hematite band is observed. A small amount of crystalline hematite (probably less than 1 wt.% based on the work of MORRIS *et al.,* 1989) may also be present in these uncommon regions; however, it would no longer be spectrally dominant.

BURNS (1993a) outlined detailed mechanisms for chemical weathering on Mars that could lead to the formation of smectites in combination with ferric oxides, oxyhydroxides, and hydroxysulfates. POLLACK *et al.* (1990) detected spectral evidence for sulfates in the airborne dust, which have been associated with the surface material on Mars. If schwertmannite were present pervasively in bright martian soil, it could account for some of the S measured by Viking (CLARK *et al.,* 1977) and for the spectral observations of POLLACK *et al.* (1990), and it would be consistent with the weathering scenarios described by BURNS (1993a). Local concentrations of schwertmannite may also be related to the uncommon bright martian regions where there is a longer-wavelength ferric absorption, although other minerals could also be responsible for this feature and there is no direct evidence for schwertmannite on Mars.

Reflectance spectra of a natural and a synthetic schwertmannite are presented here in the visible to infrared regions (0.3 to 25 μm). The spectral features in schwertmannite due to ferric species in the extended visible region and due to H_2O, OH, and sulfate complexes in the infrared region are analyzed in comparison with the spectral features of other ferric minerals, Mars soil analogs, and selected regions on Mars. As the mid-infrared spectral features are very weak in reflectance spectra of schwertmannite, transmittance spectra of schwertmannite are discussed here as well. Mössbauer spectra have been measured to provide additional information about the iron sites for interpretation of the optical spectra. Based on the visible to infrared reflectance spectra and other properties, schwertmannite is considered as a possible form of the nanophase ferric component of the bright region surface material on Mars. Remote sensing and sample analysis techniques are discussed for detecting schwertmannite, if present, in the martian surface material. Given the presence of schwertmannite or mixtures of schwertmannite and other ferric minerals, implications for the geochemistry of the surface of Mars are discussed.

BACKGROUND

Discovery of schwertmannite

Schwertmannite is an iron oxyhydroxysulfate with the empirical unit cell formula $Fe_{16}O_{16}(OH)_y(SO_4)_z \cdot nH_2O$, where $16-\mathbf{y} = 2\mathbf{z}$ and $2.0 \leq \mathbf{z} \leq 3.5$ (BIGHAM *et al.,* 1994). It was approved as an independent mineral species by the Commission on New Minerals and Mineral Names of the International Mineralogical Association in September, 1992. The first description of schwertmannite as a new mineral was published by BIGHAM *et al.* (1994). Prior to the formal approval of schwertmannite, selected data were published under the designation "mine drainage mineral" abbreviated as MDM (MURAD *et al.,* 1994).

Early studies of schwertmannite were carried out by BRADY *et al.* (1986) and MURAD (1988) before it was recognized as a discrete mineral. Lacking chemical analyses, the described phase was tentatively identified as ferrihydrite and "well"-crystallized ferrihydrite, respectively. The subsequent observation that this material always has sulfate contents from 12 to 16 wt.% led to the realization that sulfate must in some way be incorporated into the structure (BIGHAM *et al.,* 1990; MURAD *et al.,* 1990) and that it is not an iron oxyhydroxide, such

as ferrihydrite. The X-ray diffraction diagram furthermore has two peaks at higher d-spacings (0.486 and 0.339 nm) than ferrihydrite; this information was not taken into consideration in the work mentioned earlier.

Schwertmannite differs from the majority of "new" minerals in that it is not an exotic phase that exists in only a few, or even just a single locality. On the contrary, it is a mineral of relatively common occurrence in acidic environments rich in sulfate and iron. Thus, it is a typical mineral of acid mine drainage precipitates, but has also been observed to occur in totally natural environments (SCHWERTMANN *et al.*, 1995). Major complications in the identification of schwertmannite arise from its small particle size, leading to significant broadening of X-ray diffraction lines and its frequent association with other, related minerals (typically jarosite, goethite, and/or ferrihydrite). Previous studies involving "amorphous ferric gels" or similar materials from environments such as acid mine drainage may, therefore, in fact refer to schwertmannite or mineral assemblages of which schwertmannite is a constituent.

In laboratory experiments, schwertmannite has been synthesized both abiotically and under the participation of *Thiobacillus ferrooxidans*. The possibility of bacterial activity on Mars has been presented recently by FARMER (1995). Although not essential for the formation of schwertmannite, the bacterium decreases the reaction time for oxidation of sulfides and, thus, facilitates the formation of secondary precipitates. If schwertmannite is found in the martian surface material, then evidence for bacterial activity on Mars should be investigated as well (FARMER, 1995).

Characteristic properties of schwertmannite

The X-ray diffraction diagram of schwertmannite consists of eight peaks between 0.486 and 0.146 nm. The X-ray diffraction data show schwertmannite to have a structure similar to that of akaganéite (nominally ß-FeOOH), except that the *c*-dimension is doubled (BIGHAM *et al.*, 1990). In schwertmannite the sulfate is located within the approximately 0.5 × 0.5 nm wide, square tunnels that run parallel to the *c*-axis. The sulfate is, therefore, relatively readily accessible, and can be exchanged with other anions. Schwertmannite is quite stable in a dry environment, but becomes unstable when stored in an aqueous environment. A schwertmannite stored in distilled water was transformed nearly completely to goethite within a period of two months (MURAD *et al.*, 1994; BIGHAM *et al.*, 1996). Thermal transformation of schwertmannite to hematite occurs by 560°C (BIGHAM *et al.*, 1990).

Schwertmannites exhibit some variability in chemical compositions, due primarily to the extent of additional sulfate species adsorbed on the particle surfaces (BIGHAM *et al.*, 1990). The Fe/S ratio ranges from ~5–8 (BIGHAM *et al.*, 1990; SCHWERTMANN *et al.*, 1995). The purest forms of schwertmannite contain ~62–65 wt.% Fe_2O_3, ~10–13 wt.% SO_3, ~9–10 wt.% adsorbed H_2O (lost by drying at 100°C for 12–18 hours), and ~14 wt.% bound H_2O plus structural OH (lost by drying at 800°C for 12–18 hours) (BIGHAM *et al.*, 1990). As schwertmannite contains much more Fe than S, schwertmannite could not account for all of the S present in the martian soil, even if it were a major source of Fe in some regions. Other sources of S may be sulfate salts, such as $MgSO_4$ (CLARK, 1993).

Natural schwertmannites are orange to yellowish brown in color. Quantitative color measurements indicate a broad distribution of color values for natural and synthetic schwertmannite. The Munsell color hues for schwertmannite range from ~8 YR to ~2.5 Y (BIGHAM *et al.*, 1992; BIGHAM *et al.*, 1994). Schwertmannite is typically associated with other genetically related phases, which is common for many microcrystalline minerals. This may influence the color of schwertmannite, thus creating the appearance of more color variation than really exists among pure schwertmannites.

Infrared spectra taken in the wavenumber range 1800–400 cm^{-1} show a number of bands that can be assigned to SO_4 (BIGHAM *et al.*, 1990). The position of these IR bands, combined with the XRD data, provide information about the structure of schwertmannite. BIGHAM *et al.* (1990) showed that about half of the $FeO_3(OH)_3$ octahedra in the akaganéite structure are replaced by $FeO_3(OH)_2O—SO_3$ in schwertmannite. Infrared spectra have also been used to demonstrate the exchange of SO_4 by other anions, *e.g.*, SeO_4 or $HAsO_4$ (MURAD *et al.*, 1994).

Electron micrographs confirm the small particle size (0.2–0.4 × 6–9 μm) indicated by X-ray diffraction line broadening, and show schwertmannite to have a fibrous morphology that has been termed "pincushion"-like by BIGHAM *et al.* (1994).

Mössbauer spectra taken at room temperature consist of broadened, somewhat asymmetric doublets. The line widths in schwertmannite spectra are high, requiring that the spectra be fitted with distributions of doublets instead of simple Lorentzian lines. Because of this asymmetry at least two distributions of quadrupole-split doublets were

necessary. The distributions proved to have similar quadrupole splittings of maximum probability (0.65 mm/s on average), but different isomer shifts (0.39 and 0.33 mm/s). These parameters are typical for trivalent iron in moderately distorted octahedral coordination in paramagnetic minerals (*e.g.*, ferric oxides or oxyhydroxides above their respective Néel temperatures) or in superparamagnetic minerals (*e.g.*, ferric oxides or oxyhydroxides of small particle size). Thus, they do not differ sufficiently from those of numerous other minerals with which schwertmannite may be associated (*e.g.*, jarosite and ferric oxides) to allow the identification of schwertmannite in assemblages of such minerals on the basis of Mössbauer spectra taken in the paramagnetic state (see Table 1).

Mössbauer spectra taken at low temperatures have shown schwertmannite to order magnetically at 75 ± 5 K. Although the small particle size suggests that superparamagnetism could play a role in determining the magnetic properties of schwertmannite, Mössbauer spectra taken under external magnetic fields show the above temperature to correspond to a genuine Néel point. At 4.2 K the Mössbauer spectra of schwertmannite are again asymmetric and require fits entailing two distributions of magnetic hyperfine fields. Both distributions, however, have similar hyperfine fields of maximum probability of about 45.4 T. This is lower than that observed for any iron oxide or oxyhydroxide (MURAD and JOHNSTON, 1987; MURAD, 1996), and will usually allow distinction between schwertmannite and other minerals at 4.2 K (MURAD *et al.*, 1994). A summary of the Möss-

Table 1a. Average Mössbauer parameters of schwertmannite and other ferric minerals

Mineral	Room temperature			4.2 K			Néel or Curie Temperature (K)
	IS (mm/s)	QS (mm/s)	B_{hf} (T)	IS (mm/s)	QS (mm/s)	B_{hf} (T)	
Goethite[1,2]	0.37	-0.26	38.0	0.48	-0.25	50.6	400
Akaganéite[1,2]	0.37 0.38	0.55 0.95	— —	0.50 0.48 0.49	-0.02 -0.24 -0.81	48.9 47.8 47.3	299
Lepidocrocite[1,2]	0.37	0.53	—	0.47	0.02	45.8	77
Feroxyhite[1,2]	0.37	-0.06	41	0.48	~0	52 53	450
Ferrihydrite[1,2]	0.35	0.62 to 0.78	—	0.48	-0.02 to -0.07	47 to 50	25 - 115*
Hematite[1,2](wfm) (afm)	0.37	-0.20	51.8	0.49 0.49	-0.20 or 0.41	53.5 or 54.2	955
Maghemite[1,2]	0.23 0.35	≤|0.02| ≤|0.02|	50.0 50.0	0.36 0.48	≤|0.02| ≤|0.02|	53.0 52.0	~950
Jarosite[3,4]	0.37	1.16	—	0.49	0.11	49.2	54
Schwertmannite[5,6]	0.39 0.33	0.65	—	0.49	-0.35 -0.04	45.4	75

Table 1b. Average Mössbauer parameters of chemically-treated montmorillonites containing nanophase ferric minerals

Mineral	Room temperature			4.2 K		
	IS (mm/s)	QS (mm/s)	B_{hf} (T)	IS (mm/s)	QS (mm/s)	B_{hf} (T)
Ferrihydrite-bearing montmorillonite †,[3]	0.35	0.6 to 0.8	—	0.47 0.48	0.57 -0.1	48
Ferric sulfate-bearing montmorillonite †,[3]	0.37	0.7	—	0.47 0.54 0.48	0.57 -0.1 -0.2	48 45

[1] MURAD and JOHNSTON (1987), [2] MURAD (1996) and references therein. [3] BISHOP *et al.* (1995), [4] AFANASEV *et al.* (1974), [5] MURAD *et al.* (1990), [6] BIGHAM *et al.* (1994).

* Superparamagnetic blocking temperature. This varies as a function of particle size.

† Low-temperature Mössbauer spectra of chemically-treated smectites have a doublet due to structural iron (shown on the first line) and one or more sextets due to interlayer iron (shown on the following line(s)); the values given are averages for several samples.

bauer parameters of schwertmannite and other ferric minerals is provided in Table 1a, and of Mars soil analogs in Table 1b. The Mössbauer parameters listed in Table 1a are average values for crystalline materials. It should be noted that the magnetic hyperfine fields decrease with decreasing crystallinity and particle size (*e.g.,* MURAD and JOHNSTON, 1987), and that the values given in Table 1a are those of pure, bulk minerals. Schwertmannite and ferrihydrite are nanophase minerals, which should be taken into consideration when comparing their Mössbauer parameters with those of other materials.

Martian climate and surface material

The runoff and outflow channels on Mars provide evidence for abundant water there in the past (CARR, 1981). Climatic models describing a warm and wet early Mars were developed in order to explain these features (*e.g.,* POLLACK *et al.,* 1987; FANALE *et al.,* 1992). Current temperatures on Mars range from 130 to 290 K, varying both diurnally and regionally across the surface (KIEFFER *et al.,* 1977). The hypothesis of a warm and wet early Mars has been challenged recently due to a lack of spectral evidence for carbonates in the martian surface material, re-calculation of greenhouse models, proposed new methods of valley network formation, and the possibility of recent network formation or glaciation events (CARR, 1995 and references therein). Recent analyses of the valley networks and channels on Mars suggest that these features formed primarily by mass wasting and groundwater seepage (CARR, 1995). Seasonal variations in martian atmospheric water vapor levels also support the presence of near-surface reservoirs of water or ice in the regolith (JAKOSKY and HABERLE, 1992). Each of these models includes water in some form that would enable the kinds of weathering processes necessary for the formation of schwertmannite and other ferric minerals.

Geochemical results of the Viking missions led CLARK *et al.* (1977) and TOULMIN *et al.* (1977) to propose a mixture of smectites, sulfates, carbonates, and oxides as the fine-grained surface material covering Mars. Given liquid water on early Mars, chemical weathering processes and thermodynamic considerations indicate that smectites and sulfate minerals could have formed at that time, and that they would be stable under the arid conditions found today on Mars (GOODING, 1978; GOODING and KEIL, 1978; GOODING *et al.,* 1992; BURNS and FISHER, 1993). Current models of the surface material on Mars include smectite clays and clay-like mineraloids, such as palagonitic soils (BANIN *et al.,* 1992; GOODING *et al.,* 1992). The abundance of Fe and S in the martian soil, the oxidizing conditions on the surface of the planet, and the chemical reactivity of ferric species and sulfates imply that hydrated ferric sulfate minerals may have formed on Mars (BURNS, 1987, 1988, 1994; BURNS and FISHER, 1993).

Reflectance spectroscopy

Mars—The spectra of the bright regions on Mars are characterized by gently sloping ferric bands in the extended visible region (ADAMS and MCCORD, 1969; SINGER *et al.,* 1979; BELL *et al.,* 1990), weak features near 2.2–2.3 μm (MCCORD *et al.,* 1978; CLARK *et al.,* 1990; ARNOLD, 1992; MURCHIE *et al.,* 1993; BELL and CRISP, 1993; BELL *et al.,* 1994; BEINROTH and ARNOLD, 1996), a strong and broad bound water band at ~3 μm (HOUCK *et al.,* 1973; PIMENTEL *et al.,* 1974; BLANEY and MCCORD, 1989; BIBRING *et al.,* 1990; ERARD *et al.,* 1991), the possibility of a weak sulfate feature near 4.5 μm (BLANEY and MCCORD, 1995), and broad silicate emittance maxima near 10 and 20 μm (HANEL *et al.,* 1972; HUNT *et al.,* 1973). Recent reviews of the visible to infrared spectral features of Mars can be found in SODERBLOM (1992) and ROUSH *et al.* (1993).

Variations in the spectral character of Mars have been observed spatially across bright regions of the surface in the extended visible region (MCCORD *et al.,* 1977; SINGER, 1982; BELL, 1992). Specifically, Fe^{3+} transition bands are observed near 0.84–0.86 μm in the Tharsis region (BELL *et al.,* 1990), near 0.88 μm in Lunae Planum (MCCORD *et al.,* 1977; MURCHIE *et al.,* 1993), and near 0.92 μm in some of the bright soils throughout Arabia (MCCORD *et al.,* 1982; MURCHIE *et al.,* 1993).

Ferric Minerals—Reflectance spectroscopy has been measured in the visible and infrared regions of a number of ferric oxides, oxyhydroxides, and hydrated sulfates. Extended visible region reflectance spectra have been analyzed for numerous ferric minerals that have been characterized with Mössbauer spectra and other techniques (SHERMAN *et al.,* 1982; SHERMAN and WAITE, 1985; MORRIS *et al.,* 1985; BISHOP *et al.,* 1993). SHERMAN *et al.* (1982) assigned Fe^{3+} crystal field theory bands and Fe—O charge transfer bands to these visible reflectance spectra and to spectra from Mars. Ferric oxides composed of face-sharing $[FeO_6]$ octahedra also exhibit the paired Fe^{3+} transition: $^6A_1 + {}^6A_1, \rightarrow {}^4T_1 + {}^4T_1$ near 0.5 μm, which is present, but much weaker, in ferric oxyhydroxides (SHERMAN and

WAITE, 1985; BURNS, 1993b). The intensity of this paired transition decreases, as well, with decreasing particle size and substitutions of Al^{3+} for Fe^{3+} (MORRIS *et al.*, 1989, 1992; MORRIS and LAUER, 1990). Table 2a includes a summary of the extended visible region spectral properties of several ferric minerals. Detailed analyses of the crystal field theory absorptions in mineral spectra are available in BURNS (1993b).

Chemically-treated montmorillonites—Reflectance spectra of cation-exchanged montmorillonites and montmorillonites bearing hydrated ferric oxides and sulfates, such as ferrihydrite and schwertmannite, have been studied in detail by BISHOP *et al.* (1993, 1994, 1995). The ferrihydrite-bearing and ferric sulfate-bearing montmorillonites were prepared in the laboratory as analog materials for the soils in the bright regions on Mars. Reflectance spectra of these samples include gently sloping, extended visible region ferric features, bound H_2O features near 1.4, 1.9, 3, and 6 μm, cation—OH bands near 1.41, 2.75, and 10–12 μm, and broad silicate features near 10 and 20 μm. The extended visible region spectral properties of these Mars soil analog materials are summarized in Table 2b.

EXPERIMENTAL PROCEDURES

Sample preparation or location

Schwertmannite—Two schwertmannite samples are included in these analyses—a natural sample collected near Glenn's run, Belmont Co., Ohio, and a synthetic sample. Sample Bt-4 is an almost pure schwertmannite, formed at pH 3.2 in a creek that is contaminated with acid mine

Table 2a. Spectroscopic properties of schwertmannite and other ferric minerals

	Band minimum	Band maximum	Band minimum	Reference
Schwertmannite (Bt-4)		0.740	0.915	this work
Schwertmannite (Z510b)		0.730	0.918	this work
Lepidocrocite	0.65		0.96	1
	0.70	0.82	0.98	2
		0.79	~0.94	3
Maghemite			0.93	1
		~0.78	0.92-0.94	2
Goethite	~0.64		0.91-0.93	1
	~0.65	~0.76	0.92-0.94	2
		0.765	0.91	3
Ferrihydrite			0.91	1
		0.80	0.93	3
Jarosite		0.74	0.905	this work
Akaganéite			0.908	1
		0.73	0.90	3
Feroxyhite			0.88	1
		0.76	0.88	3
Hematite			0.86-0.88	1
	0.63-0.64	0.74-0.76	0.85-0.87	2
		~0.75	0.86	3

Table 2b. Spectroscopic properties of chemically-treated montmorillonites containing nanophase ferric minerals

	Band maximum	Band minimum	Reference
Ferrihydrite bearing-montmorillonite	0.77-0.80	0.89-0.92	3,4
Ferric sulfate bearing-montmorillonite	0.74-0.75	0.88-0.89	4

[1] SHERMAN *et al.* (1982). [2] MORRIS *et al.* (1985). [3] BISHOP *et al.* (1993). [4] BISHOP *et al.* (1995).

drainage precipitates (BIGHAM *et al.*, 1990). Sample Z510b is a synthetic schwertmannite formed in the laboratory at pH 2.9 under the participation of *Thiobacillus ferrooxidans* (BIGHAM *et al.*, 1990). Chemical analyses of these samples are available in BIGHAM *et al.* (1990). A portion of the natural sample was dry sieved to less than 45 μm; reflectance spectra were measured of both the bulk and <45 μm particle size samples for Bt-4. Sample Z510b was only measured as a bulk sample. These particle size separates indicate the size of aggregates of individual grains, which are much smaller.

Ferric oxides—Goethite (α—FeOOH), akaganéite (β—FeOOH), feroxyhite (δ'—FeOOH), ferrihydrite ($Fe_5HO_8 \cdot 4H_2O$), and hematite (α-Fe_2O_3) samples were collected or synthesized for an earlier study (SHERMAN *et al.*, 1982). A previously studied natural specimen of magnetite (Fe_3O_4) from Grangeburg, NY (BISHOP *et al.*, 1993) and a previously studied jarosite ($KFe_3(SO_4)_2(OH)_6$) sample (BURNS, 1987) are included here. Insufficient quantity of these samples was available to separate them by particle size. The aggregated particle sizes were estimated by visual inspection at approximately less than 125 μm.

Goethite, lepidocrocite (γ—FeOOH), and ferrihydrite were synthesized following procedures described in SCHWERTMANN and CORNELL (1991) for a previous study (BISHOP *et al.*, 1993). These samples were dry sieved to less than 45 μm.

Chemically-treated montmorillonites—SWy-1 montmorillonite (The Clay Minerals Society, Source Clay Minerals Repository) normally contains Na and Ca cations in the interlayer sites. This natural montmorillonite has been chemically treated in the laboratory to produce montmorillonites containing a variety of interlayer ferric complexes. Ferric-doped montmorillonites have been produced and studied in many laboratories (BISHOP *et al.*, 1993, 1995; BANIN and RISHPON, 1979; BANIN *et al.* 1988; ORENBERG and HANDY, 1992). Low-temperature Mössbauer spectra of the samples prepared by BISHOP *et al.* (1993) have strong similarities with the mineral ferrihydrite and have been therefore named ferrihydrite-montmorillonite assemblages or ferrihydrite-bearing montmorillonites. The ferric sulfate-bearing montmorillonites were prepared by adding ferric sulfate solution to a protonated montmorillonite suspension under low pH (1.6–1.8), then raising the pH to 3.0–4.0, depending on the sample (BISHOP *et al.*, 1995). These samples were dry sieved to less than 45 μm; the actual grain sizes of the natural and chemically-treated montmorillonites are on the order of 1–2 μm.

Reflectance spectroscopy

Spectra were measured relative to Halon from 0.3 to 3.6 μm under ambient conditions with the RELAB (reflectance experiment laboratory) spectrometer at Brown University. The Halon spectrum is multiplied by wavelength- and angle-dependent correction factors, giving absolute reflectance values for the samples. A photomultiplier tube is used for the visible to near-infrared region and an InSb detector is used for the infrared region. This instrument has been described in detail in PIETERS (1983). The RELAB spectrometer allows for variable illumination (i) and emergence (e) angles. Spectra included here were measured at i = 30° and e = 0°. The sample dish is rotated during the measurement to eliminate orientation effects.

Infrared reflectance spectra were measured relative to a rough gold surface, using a Nicolet 740 Fourier transform interferometer (FTIR), in an H_2O- and CO_2(g)-purged environment. A PbSe detector was used in the range 0.9 μm to 3.2 μm and a DTGS (deuterated triglycine sulfate) detector between 1.6 μm and 25 μm. The sample chamber, including a remotely controlled sample train, was manufactured by SpectraTech and uses a biconical arrangement. Composite spectra were prepared by splicing RELAB data at 1.2 μm with Nicolet data (1.2 μm to 25 μm). The Nicolet spectra were scaled to those measured using the RELAB spectrometer.

Sample preparation for the spectral measurements involved pouring the particulate material into a sample dish 12 mm in diameter and 3 mm in depth. The dish was tapped gently on a hard surface to settle the particles, then re-filled. This procedure was continued until the dish remained full. The sample surface was not smoothed with a spatula. For measurement of some of the ferric minerals, where very small amounts of material were available, it was necessary to use smaller sample dishes.

Additional infrared reflectance spectra were measured using a Nicolet Magna 550 FTIR spectrometer with a DTGS detector and a Harrick "Drift" sample measurement system at the Bayerisches Geologisches Landesamt in Bamberg. In order to give absolute reflectance, these spectra were scaled at 1390 cm^{-1} to the reflectance spectra obtained at Brown University.

Transmittance spectroscopy

Infrared transmittance spectra were measured in the range 400 to 4000 cm^{-1} (2.5 to 25 μm) using a Nicolet Magna 550 FTIR spectrometer with a DTGS detector. One mg of sample was pressed between two KBr disks (but not mixed with KBr, thus avoiding reaction between the schwertmannite and KBr). A KBr pressed pellet was prepared as a blank standard. Additional spectra were obtained by attenuated total reflectance using an ATR kit equipped with a ZnSe plate. Peak positions of the spectral features were determined either directly or from first derivatives using the Nicolet OMNIC software.

Mössbauer spectroscopy

Mössbauer spectra of sample Bt-4 were taken at 295 and 4.2 K using a ^{57}Co/Rh source. In order to obtain a homogeneous iron distribution, the sample was mixed with 2 parts sugar and placed in a sample holder with an area of 2 cm^2. The transmitted radiation was recorded with a proportional counter and stored in a 1024 channel analyzer. A metallic Fe foil was used for velocity calibration and as an isomer shift reference. The room-temperature spectrum was taken in the velocity range ± 2 mm/s on a sample containing 20 mg schwertmannite until 3.6×10^6 counts per channel had been accumulated. The spectrum at 4.2 K was taken in the velocity range ± 10.6 mm/s on a sample containing 36 mg schwertmannite, cooling both source and absorber in a bath cryostat, until 4.7×10^6 counts per channel had been accumulated. The mirror halves of the spectra were folded and fitted with distributions of Lorentzian lines by a computer procedure, constraining corresponding lines of every doublet and sextet to have equal widths and intensities. This fitting procedure has been described in more detail by MURAD (1988).

RESULTS

The spectral properties of schwertmannite are presented here, with a focus on reflectance spec-

troscopy because that is the primary means at this time of gaining spectral information from Mars. As schwertmannite is a fine-grained mineral, many of the mid-range infrared spectral features are weak and difficult to interpret. In order to understand the origin of the spectral features and gain additional information about the mineral structure, transmittance spectra are evaluated in this region as well. The character of the Fe^{3+} sites in schwertmannite and the nature of the Fe—O bonds are responsible for the dominant extended visible region features in the reflectance spectra of schwertmannite. Mössbauer spectra also provide information about these Fe^{3+} sites, and are, therefore, analyzed here in combination with the optical spectra.

Reflectance spectroscopy—extended visible region

The reflectance spectrum of a natural schwertmannite (sample Bt-4) is shown in Fig. 1 from 0.3–1.3 μm (~30,000–8000 cm^{-1}) along with spectra of several other ferric minerals. The spectrum of schwertmannite exhibits a steep absorption edge beginning at about 0.5 μm, a gently sloping shoulder near 0.6 μm, a local reflectance maximum near 0.74 μm and a broad absorption band with a minimum near 0.91 μm. Included in Fig. 1 are spectra of akaganéite and jarosite that exhibit a local reflectance maximum near 0.73–0.74 μm and an absorption feature with a minimum near 0.90 μm. The positions of these reflectance maxima and minima in the schwertmannite spectrum in this region resemble more closely the spectral character of akaganéite and jarosite than those of other ferric minerals shown in Fig. 1. The broadness of the ferric transition near 0.91 μm in the spectrum of schwertmannite is similar to that of ferrihydrite, although for ferrihydrite this band occurs at a longer wavelength.

In Fig. 2 are shown extended visible region reflectance spectra of two schwertmannite samples, and chemically-treated montmorillonites containing ferric sulfate species and ferrihydrite. The spectral properties of the natural (Bt-4) and synthetic (Z510b) schwertmannites shown in Fig. 2 are in general similar, although subtle differences are present in the reflectance spectra of these two samples in this region. For example, the ferric band near 0.91 μm in the spectrum of the synthetic schwertmannite is deeper than the band in the natural schwertmannite spectrum. First derivatives of the spectra give local reflectance maxima of 0.740 μm for the natural schwertmannite Bt-4 and 0.730 μm for the synthetic schwertmannite Z510b and

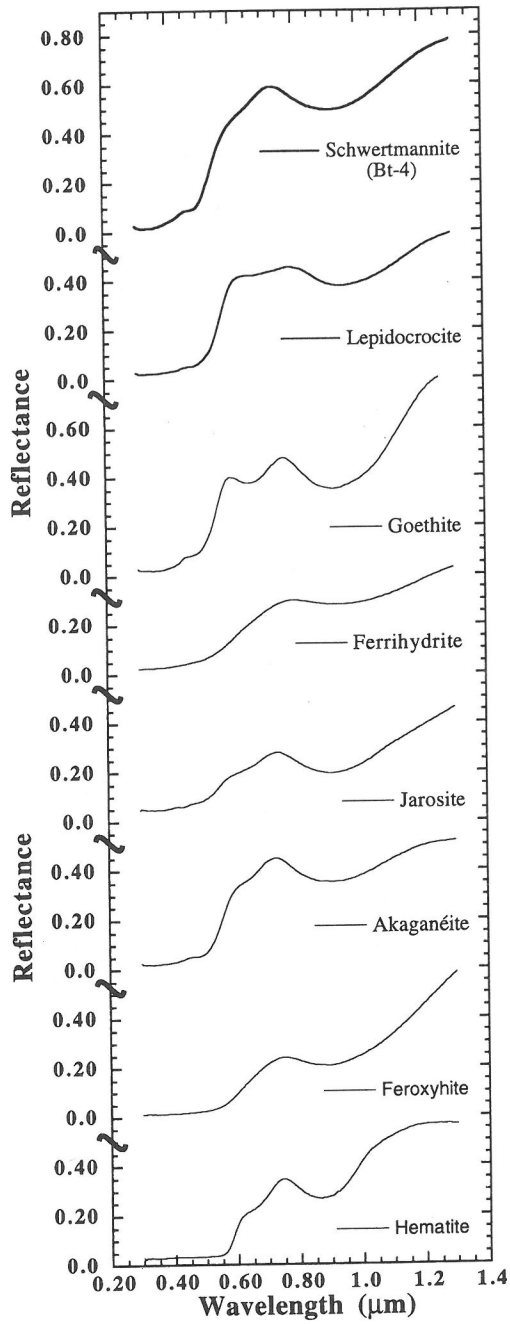

FIG. 1 Reflectance spectra of schwertmannite and ferric minerals in the extended visible region (0.3–1.3 μm). The ferric oxides and oxyhydroxides are arranged in approximate order of the position of their ferric band near 0.9 μm.

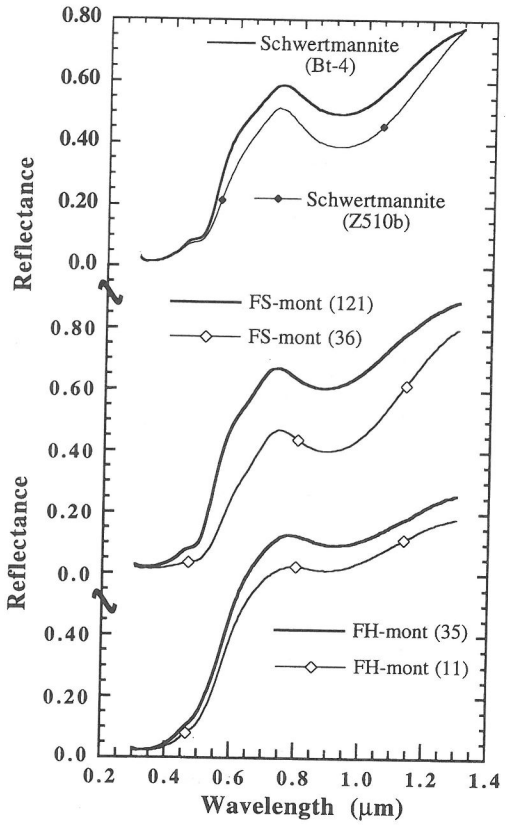

FIG. 2 Reflectance spectra of natural and synthetic schwertmannites and Mars soils analogs in the extended visible region (0.3–1.3 μm). Spectra of two ferrihydrite-bearing montmorillonites (FH-mont) and two ferric sulfate-bearing montmorillonites (FS-mont) are also shown here for comparison.

local reflectance minima at 0.915 μm for sample Bt-4 and 0.918 μm for sample Z510b. The ferric absorption occurs near 0.91–0.92 μm in spectra of the ferrihydrite-bearing montmorillonites and near 0.88–0.89 μm in spectra of the ferric sulfate-bearing montmorillonites shown in Fig. 2.

Mössbauer spectroscopy

Mössbauer spectra of sample Bt-4 measured at room temperature and at 4.2 K are shown in Figs. 3a and b, respectively. These spectra exhibit the characteristic features of all schwertmannites: broad asymmetric doublets at room temperature (Fig. 3a) and broad, asymmetric sextets at 4.2 K (Fig. 3b). The room-temperature spectrum was fitted with two distributions of quadrupole-split doublets of different isomer shifts (0.33 and 0.39 mm/s); both distributions have a quadrupole splitting value with a maximum probability of 0.68 mm/s. The spectrum taken at 4.2 K was fitted with two distributions of sextets with different quadrupole interactions (−0.03 and −0.33 mm/s); the magnetic hyperfine fields of maximum probability were 44.9 and 45.0 T, which are somewhat lower than the averge values for schwertmannite given in Table 1a. These parameters for sample Bt-4 lie within the range of values reported for other, natural and synthetic, schwertmannites (MURAD *et al.*, 1990; BIGHAM *et al.*, 1990). Average values of IS, QS, and B_{hf} for several schwertmannites are shown in Table 1. No Mössbauer data are available for sample Z510b; however, substantial Mössbauer data have been published on sample Z500a, a synthetic sample prepared by the same procedure as for Z510b (MURAD, 1988; MURAD *et al.*, 1990; BIGHAM *et al.*, 1990).

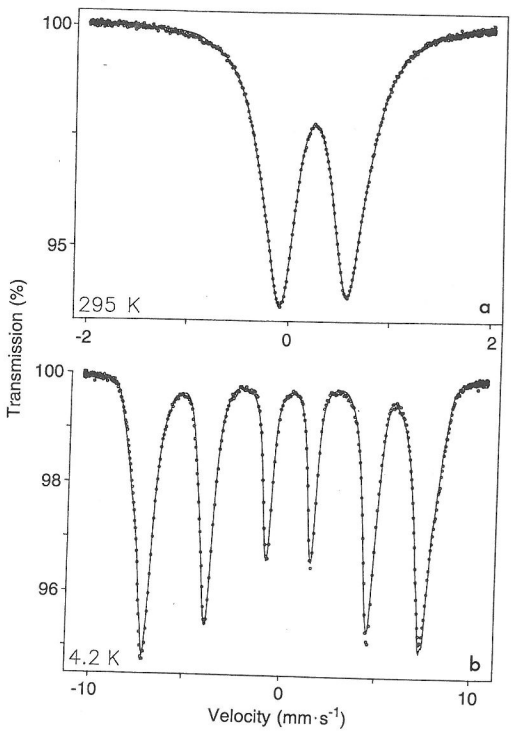

FIG. 3 Mössbauer spectra of the natural schwertmannite sample Bt-4 measured at (a) room temperature and (b) 4.2 K. Fits of the room-temperature spectrum resulted in two distributions of Lorentzian-split doublets that differ in their isomer shifts. For the spectrum taken at 4.2 K the best fit includes two distributions of magnetic hyperfine fields with different quadrupole interactions.

Reflectance spectroscopy—near infrared region

Near-infrared (NIR) reflectance spectra of the natural schwertmannite Bt-4 and the synthetic schwertmannite Z510b are shown in Fig. 4a. The synthetic schwertmannite sample exhibits darker reflectance values than the natural sample in the visible to near-infrared region, except for the range 1.3–1.4 μm. The spectra of each of these schwertmannites contain broad features due to bound H_2O near 1.45 μm, 1.95 μm, and near 3 μm. The schwertmannite spectra were measured in a dry environment (the air in the sample chamber was purged of water and CO_2 for more than 12 hours), where all or most of the adsorbed water was removed from the sample.

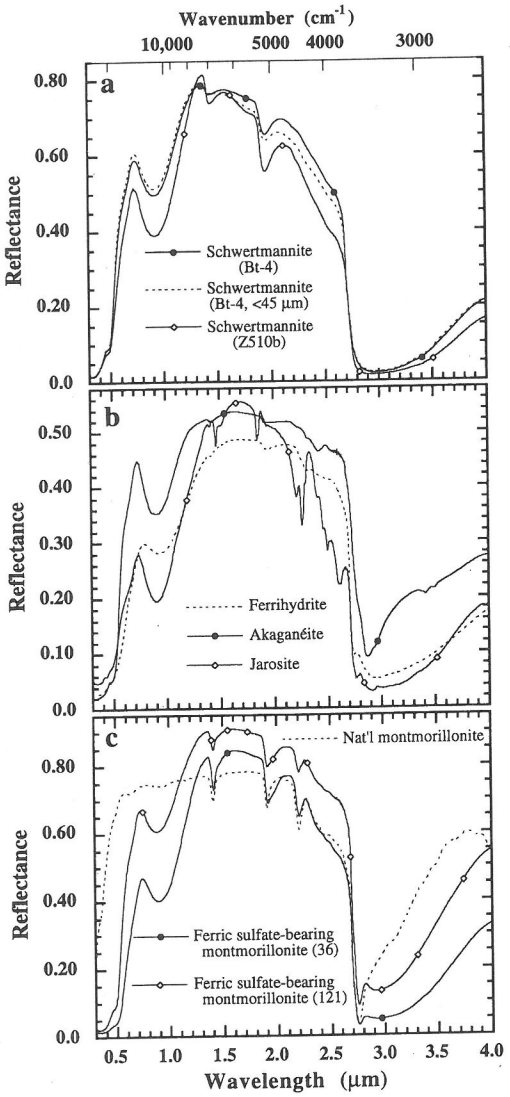

FIG. 4 Reflectance spectra in the visible to near-infrared region (0.3–4.0 μm): a) natural (Bt-4) and synthetic (Z510b) schwertmannite, b) akaganéite, jarosite, and ferrihydrite, and c) natural SWy-1 montmorillonite and two ferric sulfate-bearing montmorillonites.

Near-infrared reflectance spectra of ferrihydrite, akaganéite, and jarosite are shown in Fig. 4b for comparison to schwertmannite. Although the spectral properties of these three ferric minerals are similar to those of schwertmannite in the extended visible region, they exhibit significant differences in the near-infrared region. The reflectance spectra of schwertmannite in this region are much brighter and have a stronger negative continuum slope from ~1.4 to 2.5 μm. The jarosite spectrum has narrow features near 1.4, 1.9, 2.2–2.3, and 2.75 μm due to structural OH species and additional features near 2.6 μm due to combinations of OH or O—H—O vibrations (GAFFEY *et al.*, 1993). Weak absorption features are observed in the spectrum of akaganéite near 1.45 and 1.95 μm due to bound water, and near 2.4 μm probably due to structural OH. The broad, bound H_2O features observed in the spectrum of ferrihydrite are similar to those seen in the spectra of schwertmannite (Fig. 4a).

Reflectance spectra of natural SWy-1 montmorillonite and two ferric sulfate-bearing montmorillonites are shown in Fig. 4c. Several spectral changes can be seen as a result of the chemical treatment of the natural montmorillonite. The spectra of the ferric sulfate-bearing samples exhibit intense ferric features near 0.9 μm and a broad, bound water feature near 3 μm. The spectrum of the natural montmorillonite exhibits narrow features near 1.41 and 1.91 μm, while broad shoulders near 1.45 and 1.97 μm are observed in the spectra of the ferric sulfate-bearing montmorillonites. These broad, bound water features are similar to those observed in spectra of ferrihydrite and schwertmannite.

Reflectance spectroscopy—mid-infrared region

Reflectance spectra are shown as a function of wavenumber from 3330 to 400 cm^{-1} (~3–25 μm) in Fig. 5a for natural and synthetic schwertmannite. The primary absorption features in the reflectance spectrum of schwertmannite in this region occur near 3000 cm^{-1} (~3–3.5 μm) and 1640 cm^{-1} (6.1 μm) and are due to bound water. A reflectance minimum (also called Christiansen feature, see below) occurs near 1200 cm^{-1} (8.3 μm) and weaker features are observed near 1150 cm^{-1} (8.7 μm), 1060 cm^{-1} (9.4 μm), 985 cm^{-1} (10.2 μm), ~730

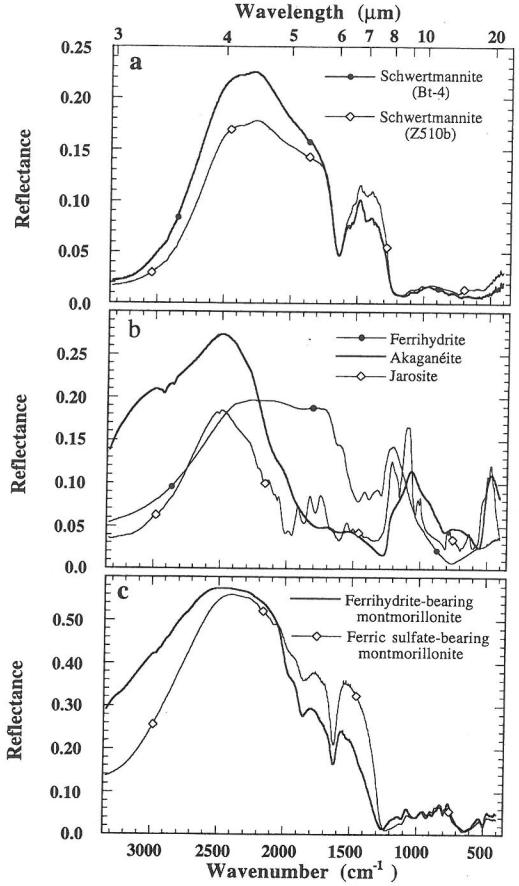

FIG. 5 Reflectance spectra in the mid-infrared region (3330–400 cm^{-1} or ~3–25 μm): a) natural (Bt-4) and synthetic (Z510b) schwertmannite, b) akaganéite, jarosite, and ferrihydrite, and c) ferrihydrite-bearing montmorillonite and ferric sulfate-bearing montmorillonite.

cm^{-1} (13.7 μm), 630 cm^{-1} (15.9 μm), and 565 cm^{-1} (17.7 μm) in the spectra of schwertmannite and differ somewhat for the two samples measured here. These bands are summarized in Table 3. A few weak and poorly resolved features in the range 1350–1550 cm^{-1} (~6.4–7.4 μm) are attributed to a minor amount of jarosite. Weak features, observed near 915 cm^{-1} (10.9 μm) and 800 cm^{-1} (12.5 μm) in Bt-4, are also assigned to impurities in this sample.

Mid-infrared reflectance spectra are shown in Fig. 5b of ferrihydrite, akaganéite, and jarosite. The spectrum of schwertmannite in this region (Fig. 5a) is much darker than the spectra of ferrihydrite, akaganéite, and jarosite. The Christiansen feature is a strong reflectance minimum that is associated with the principal molecular vibration in silicates (SALISBURY, 1993) and occurs where the real part of the index of refraction, n, approaches that of the surrounding medium, generally unity (CONEL, 1969). This has been measured for a number of geological samples and may be useful in remote characterization of planetary surfaces (SALISBURY, 1993). This reflectance minimum occurs near 1400 cm^{-1} (~7.1 μm) for jarosite, near 1280 cm^{-1} (~7.8 μm) for akaganéite; in both cases at shorter wavelengths than for schwertmannite.

Reflectance spectra of a ferric sulfate-bearing montmorillonite and a ferrihydrite-bearing montmorillonite are displayed in Fig. 5c. The feature near 1635 cm^{-1} in these spectra is due to bound H_2O. The Christiansen feature occurs as a broad reflectance minimum at 1240–1255 cm^{-1} (~8 μm) for ferrihydrite-bearing montmorillonites and at 1210–1250 cm^{-1} (~8–8.3 μm) for ferric sulfate-bearing montmorillonites. In the scattering regime, at wavelengths longer than the Christiansen feature, these spectra are very dark and exhibit weak features, much like the spectra of schwertmannite in Fig. 5a.

Transmittance and ATR spectroscopy

Transmittance spectra of samples Bt-4 and Z510b were measured from 4000 to 400 cm^{-1} (2.5–25 μm) and ATR spectra from 4000 to 630 cm^{-1} (2.5–16 μm). These are shown in Fig. 6 from 1300 to 400 cm^{-1} (7.7–25 μm). A strong, broad spectral band near 3300 cm^{-1} (~3 μm) and another feature at ~1630 cm^{-1} (6.14 μm) due to water are observed in these spectra, but are not shown in Fig. 6. Additional spectral features are observed at approximately 1180 cm^{-1} (8.5 μm), 1100 cm^{-1} (9.1 μm), 1045 cm^{-1} (9.6 μm), 980 cm^{-1} (10.2 μm), 800–850 cm^{-1} (12.5–12 μm), 700 cm^{-1} (14.3 μm), 610 cm^{-1} (16.4 μm), 520 cm^{-1} (19.2 μm), 465 cm^{-1} (21.5 μm), and 415 cm^{-1} (24.1 μm) (Table 3). Subtle differences in the strengths and positions of these features can be seen in Fig. 6 for the two schwertmannite samples studied here. Band assignments for the mid-IR transmittance features of schwertmannite are listed in Table 3. The features due to impurities found in the reflectance spectra are either absent or much weaker in the transmittance spectra of schwertmannite.

DISCUSSION

Spectral features due to ferric iron

The spectral character of ferric minerals in the extended visible region is dominated by ferric crystal field theory bands (SHERMAN *et al.*, 1982; SHER-

Table 3. Infrared absorptions in spectra of natural (Bt-4) and synthetic (Z510b) schwertmannites

Transmittance **Bt-4** (cm^{-1})	Reflectance **Bt-4** (cm^{-1})	Transmittance **Z510b** (cm^{-1})	Reflectance **Z510b** (cm^{-1})	Band Assignment
~1635	~1640	~1630	~1640	bound H_2O bend[1]
~1180†	~1200†	~1190†	~1210†	ν_3 sulfate vib. or ν_4 acid sulfate vib.[2]
~1100	~1140	~1120	~1150	ν_3 sulfate asymmetric stretch[1,2]
~1045	~1060	~1070	~1060	ν_3 sulfate asymmetric stretch[1,2] or ν_2 acid sulfate vib.[2]
~980	~985	~980	~985	ν_1 sulfate symmetric stretch[1]
~800-850*		~800-850		OH bend[1,2]
~700	~720	~700	~735	OH bend[2]
~610	(620)†	~610	~630	ν_4 sulfate asymmetric bend[1,2]
~520	(565)†	(520)†	~565	ν_2 or ν_4 sulfate bend or acid sulfate bend[2]
~465		(465)†		ν_2 sulfate symmetric bend[2]
~415	~400-420	~420	~400-420	Fe-O stretch[1,2]

[1] BIGHAM *et al.* (1990), BIGHAM *et al.* (1994).
[2] Based on assignments for other ferric sulfate minerals in Farmer (1974).
* This band is partially masked by weak features due to a small amount of goethite in the sample.
† Probable location of band centers; bands are broad or weak.
Note: All transmission features above 650 cm^{-1} were confirmed by ATR.

MAN and WAITE, 1985; BURNS, 1993b). The absorption edge near 0.5 μm, due to the $^6A_1 + {}^6A_1 \rightarrow {}^4T_1 + {}^4T_1$ paired transition, is evident in the spectra of schwertmannite, as well as in spectra of the other ferric minerals (Figs. 1 and 2). A poorly-defined shoulder near 0.6 μm is due to a weak $^6A_1 \rightarrow {}^4T_2$ transition that is angular in the spectra of akaganéite, goethite, and hematite shown in Fig. 1. The broadness of the $^6A_1 \rightarrow {}^4T_1$ band near 0.91 μm is consistent with multiple Fe^{3+} sites in the structure of schwertmannite or vibronic coupling (BURNS, 1993b). Broad $^6A_1 \rightarrow {}^4T_1$ bands are also observed for akaganéite and ferrihydrite (Fig. 1). As the mineral structures of akaganéite and schwertmannite are similar, the observed reduction in the intensity of the $^6A_1 \rightarrow {}^4T_2$ absorption feature and broadening of the $^6A_1 \rightarrow {}^4T_1$ band imply that schwertmannite is less crystalline than akaganéite or that there is a broader distribution of Fe^{3+} sites in the mineral structure.

Some of the Fe^{3+} cations in schwertmannite occur in octahedral coordination with O, OH, and O—SO_3, while others are coordinated only with O and OH (BIGHAM *et al.*, 1990, 1994). Mössbauer spectra of schwertmannite measured at room temperature exhibit two isomer shift values and at 4.2 K two quadrupole splitting values. The electron density on the Fe^{3+} nuclei is sufficiently different in these two sites that two Fe^{3+} sites can be detected in the paramagnetic state. In akaganéite the Fe^{3+} cations are octahedrally coordinated to both O and OH, which gives a broad ferric $^6A_1 \rightarrow {}^4T_1$ transition located near 0.90 μm. Therefore, the O—SO_3 species in schwertmannite are probably responsible for the longer wavelength (~0.91 μm) portion of this broad band, while the $FeO_3(OH)_3$ sites would be expected to give a transition near 0.90 μm, as seen in spectra of akaganéite.

BURNS (1993b) discussed the influence of covalent bonding on the metal-ligand bond length and crystal field splitting energy (CFSE). The ligand's ability to delocalize electronic charge bears directly on the electronic environment of the metal cation and, hence, its CFSE. BURNS (1993b) described the situation for hematite and goethite as examples. The FeO_6 bonding configuration in hematite requires a higher electron density on O and lower electron density on Fe^{3+} than does the $FeO_4(OH)_2$ bonding configuration in goethite. The CFSE is higher for hematite than for goethite, and correspondingly, the ferric $6A_1 \rightarrow 4T_1$ transition occurs at a shorter wavelength for hematite than for goethite.

These results from BURNS (1993b) can be extrapolated to the structures of akaganéite and schwertmannite. The replacement of OH by O—SO_3 in some of the $FeO_3(OH)_3$ sites causes a change in the electron density distribution and degree of covalent bonding. Based on the polarizing power of the sulfate ion (*e.g.*, HUHEEY *et al.*, 1993), the SO_3 groups

are better able to delocalize the electronic charge on O than H, thus, the electron density on O will be lower for the $FeO_3(OH)_2O—SO_3$ sites than for the $FeO_3(OH)_3$ sites. Therefore, a lower CFSE and longer wavelength ferric absorption feature for the sulfate-bearing sites compared to the akaganéite-like sites in schwertmannite are predicted. This interpretation of the nature of the chemical bonds in schwertmannite is consistent with the observed optical spectra in Figs. 1 and 2.

Additional features in the mid-infrared spectral region result from ferric iron in the schwertmannite structure. These include absorption features due to Fe—O stretching vibrations, Fe—OH bending vibrations, and Fe—O—SO_3 vibrations. Strong absorption features at 704 and 483 cm^{-1} were tentatively assigned to Fe—O stretching modes in schwertmannite (Bigham *et al.*, 1994). Although Fe—O stretching vibrations do have energies in this region, OH bending vibrations and sulfate ν_2 vibrations also occur in this region for hydrated ferric sulfates (Ross, 1974). Based on the spectra discussed by Ross (1974), the absorption features observed in the transmittance spectra of schwertmannite near 700 and 465 cm^{-1} in Fig. 6 are assigned here to an OH bending mode and a ν_2 symmetric sulfate bending mode, respectively, and are discussed in more detail in the following sections. However, the lower energy absorption feature near 425–430 cm^{-1} is assigned to an Fe—O stretching mode. This Fe—O absorption feature is centered at ~415 cm^{-1} for sample Bt-4 and at ~420 cm^{-1} for sample Z510b in the transmittance spectra shown in Fig. 6.

Spectral features due to adsorbed and bound H_2O

The broad, bound H_2O features observed near 1.45, 1.95, 2.75–3.5, and 6.1 μm in the spectra of natural and synthetic schwertmannite are much stronger than these features in the akaganéite spectrum. In each case spectra were measured after H_2O and CO_2 were purged overnight from the air in the sample chamber. For smectite clays, dehydrating the samples by placing them overnight in a H_2O- and CO_2-purged sample chamber or heating them at ~100°C overnight proved effective in removing

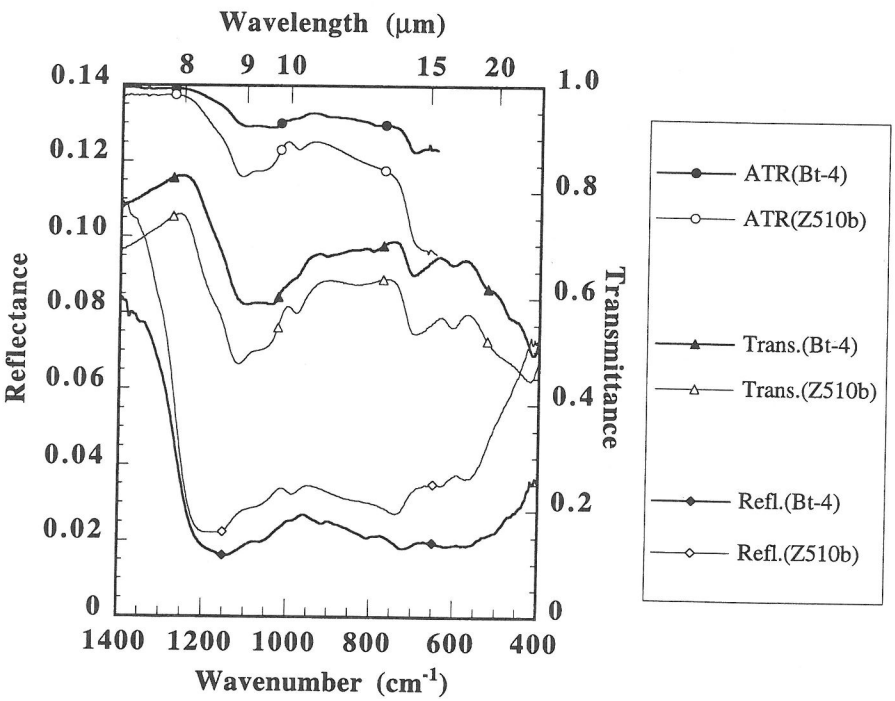

FIG. 6 Reflectance, transmittance, and attenuated total reflectance (ATR) spectra of natural and synthetic schwertmannite in the mid-infrared region (1400–400 cm^{-1} or ~7.1–25 μm). The natural schwertmannite (Bt-4) spectra are labeled with filled symbols and the synthetic schwertmannite (Z510b) spectra are labeled with open symbols.

adsorbed H_2O (Bishop *et al.*, 1994). Assuming that the adsorbed H_2O molecules in schwertmannite behave similarly to those in smectites, then the spectral features due to water in Fig. 4a are primarily due to the presence of bound water, rather than adsorbed water, in schwertmannite. The highly polarizing nature of the sulfate species causes an increase in the intensity of the spectral water features in two ways: (i) by holding additional bound water molecules in the sample and (ii) because the polarization enhances the band strength for a given amount of water molecules.

The bound water features in spectra of the ferric sulfate-bearing montmorillonites occur at longer wavelengths and are broader than the bound water features in spectra of natural montmorillonites (Fig. 4c). The broadening of these spectral features near 1.45 and 1.97 μm in the ferric sulfate-bearing montmorillonite relative to the natural montmorillonite could be due to the presence of schwertmannite. Based on low temperature Mössbauer spectroscopy and other analyses, the ferric sulfate-bearing montmorillonite samples are thought to contain both schwertmannite and ferrihydrite (Bishop *et al.*, 1995). The ferric sulfate-bearing montmorillonites, ferrihydrite, and schwertmannite all contain adsorbed and bound water under ambient conditions.

Band depths of the near-infrared features in schwertmannite are dependent on the environmental conditions and were measured here according to the method of Clark and Roush (1984). Reflectance spectra measured under ambient conditions resulted in band depths of 6 % and 19% at 1.45 and 1.95 μm, respectively, for sample Bt-4. Similarly, sample Z510b exhibited band depths of 14% and 31% for the absorption features at 1.45 and 1.95 μm, respectively. Reflectance spectra of these samples under controlled, dry conditions gave band depths of 3% and 10% at 1.45 and 1.95 μm, respectively, for sample Bt-4 and band depths of 8% and 18% at 1.45 and 1.95 μm, respectively, for sample Z510b. By assuming that the spectra measured under dehydrated conditions do not include any adsorbed water, the portion of these spectral features attributed to the adsorbed water can be roughly determined by subtracting the band depths of the ''dry'' spectra from those of the ambient spectra. This results in 3% and 9% band depths at 1.45 and 1.95 μm, respectively, due to adsorbed water in Bt-4, and 6% and 13% band depths at 1.45 and 1.95 μm, respectively, due to adsorbed water in Z510b. The differences in the near-infrared band depths of the bound water features between the two samples imply that the amount of bound water contained in the mineral schwertmannite can vary from sample to sample. This is consistent with the variability in OH and SO_4 in the schwertmannite structure (Bigham *et al.*, 1994).

The amount of water lost by heating schwertmannite samples to 100°C and 800°C was measured for several samples (Bigham *et al.*, 1990). This study determined that 8.8 wt.% H_2O was lost on heating to 100°C and an additional 11.3 wt.% H_2O was lost on heating to 800°C for sample Bt-4. Similarly, for sample Z510b, 9.8 and 14.1 wt.% H_2O were lost on heating to 100°C and 800°C, respectively. These results are consistent with the greater magnitude of the bound water absorption features observed in the near-infrared reflectance spectra of Z510b than in spectra of Bt-4 (Figure 4a). The formula for schwertmannite indicates that H_2O molecules are associated with this mineral, but that H_2O molecules are not included in the structure (Bigham *et al.*, 1994). Water must be chemisorbed or bound to the grain surfaces or in the tunnels because it is retained in the sample at elevated temperatures as shown by measurements in Bigham *et al.* (1990) and under dehydrated conditions as shown by the near-infrared spectra in Fig. 4a.

The wt.% H_2O lost upon heating to 800°C is due to a combination of bound water and structural OH. If the amount due to structural OH is assumed to be about the same in each sample, then the differences measured in wt.% H_2O lost upon heating to 800°C would be due to differences in the amount of bound water in each sample. The band depths due to bound water in smectites were found to be linearly related to the wt.% H_2O lost upon heating to 500°C (Bishop *et al.*, 1994). It can be assumed that the NIR band depths due to bound water are also linearly related to the wt.% H_2O lost upon heating of schwertmannite. The NIR bound water band depths (at 1.45 and 1.95 μm) for Z510b are roughly twice as strong as those for Bt-4. It can then be assumed that the amount of bound water lost upon heating to 800°C (as measured by Bigham *et al.*, 1990) is about twice as large for sample Z510b as for sample Bt-4. This gives approximately 8 wt.% H_2O as structural OH in both samples, ~3 wt.% H_2O as bound water in Bt-4, and ~6 wt.% H_2O as bound water in Z510b. Additional thermal and spectroscopic analyses could be used to more precisely estimate the structural OH, bound H_2O, and adsorbed H_2O components of schwertmannite.

Spectral features due to OH

A broad spectral shoulder near 2.5 μm in the schwertmannite spectra may be related to the fea-

tures from 2.4–2.6 μm in akaganéite and jarosite in Fig. 4. Spectral features in this region for sulfate minerals are assigned to combinations of the OH stretching and bending modes (*e.g.,* GAFFEY *et al.,* 1993). The broad water band near 3 μm in the spectra of schwertmannite has a steep slope and angular character near 2.75 μm that may be due to structural OH, as observed in the spectrum of jarosite (Fig. 4).

Bending modes of OH species attached to Fe^{3+} cations occur in the range ~700–900 cm^{-1} for most hydroxylated ferric minerals, but they also occur at higher energies for jarosite and a few other hydroxylated ferric sulfate minerals (FARMER, 1974). In the transmittance spectrum of sample Bt-4, Fe—OH bending modes are observed near 700, 800, and 900 cm^{-1}. The features at ~800 and ~915 cm^{-1} are very weak in comparison to the feature near 700 cm^{-1} and are not observed in the spectrum of Z510b (Fig. 6). Strong bands are observed near 800 and 900 cm^{-1} in transmittance spectra of goethite (not shown). Jarosite exhibits a spectral feature near 790 cm^{-1} and plumbojarosite has a feature at 915 cm^{-1} due to OH bending modes (ROSS, 1974). X-ray powder diffraction patterns indicate that sample Bt-4 contains a small amount (<1wt.%) of jarosite and goethite, which are not found in sample Z510b. Therefore, weak features observed near 800 and 900 cm^{-1}, are assigned to small amounts of goethite, jarosite and/or plumbojarosite in the Bt-4 schwertmannite sample. Weak features in the range 1350–1550 cm^{-1} are also assigned to small amounts of jarosite.

BIGHAM *et al.* (1994) assigned a broad, weak band from 800–880 cm^{-1} to a bending mode of OH bound to Fe^{3+} cations. A broad band centered near 800–850 cm^{-1} is observed in the transmittance spectra, but only very weakly, if at all, in the reflectance spectra of our samples. An additional feature is observed at ~700 cm^{-1} in the transmittance spectra and from 725–735 cm^{-1} in the reflectance spectra. Small differences such as these in the position of fundamental vibrations between transmittance and reflectance spectra of minerals are common (*e.g.,* SALISBURY *et al.,* 1991). We have assigned these features to an additional Fe—OH bending mode in schwertmannite. Two distinct Fe—OH bending modes are expected for schwertmannite because of two ferric sites, $FeO_3(OH)_3$ and $FeO_3(OH)_2O$—SO_3, brought on by interactions (or bridges) between the SO_4^{2-} anions and the schwertmannite structure.

Spectral features due to sulfate species

Detailed spectral analyses of hydroxylated ferric sulfates are provided by ROSS (1974). Four sulfate vibrational modes exist in infrared spectra and are defined (i) for isolated, tetrahedral (Td) SO_4^{2-} at 983 cm^{-1} as ν_1 (symmetric stretch), at 450 cm^{-1} as ν_2 (symmetric bend), at 1105 cm^{-1} as ν_3 (asymmetric stretch), and at 611 cm^{-1} as ν_4 (asymmetric bend), and (ii) for acid sulfates at 887 cm^{-1} as ν_1 (S—OH stretch), at 1051 cm^{-1} as ν_2 (SO_3 symmetric stretch), at 594 cm^{-1} as ν_3 (SO_3 symmetric bend), at 1200 cm^{-1} as ν_4 (SO_3 asymmetric stretch), at 594 cm^{-1} as ν_5 (degenerate OSO bend), and at 429 cm^{-1} as ν_6 (degenerate OH—S—O bend). The form of the sulfate species in schwertmannite is probably somewhere in between these two forms. Evidence for these spectral modes is observed in schwertmannite spectra (Fig. 6) and summarized in Table 3 for the samples measured here.

Numerous spectral bands due to SO_4^{2-} species have been observed in several schwertmannite and related samples in the mid-infrared region (BIGHAM *et al.,* 1990, 1994). The strength and presence of these features was found to be dependent on the crystallinity of the sample (BIGHAM *et al.,* 1990) and band assignments were made for an absorption feature at 976 cm^{-1} to the ν_1 mode, for three bands at 1186, 1124, and 1038 cm^{-1} to a splitting of the ν_3 mode, and for a feature at 608 cm^{-1} to the ν_4 mode (BIGHAM *et al.,* 1994).

The spectra of samples Bt-4 and Z510b shown in Fig. 6 exhibit a strong ν_3 sulfate vibration near 1100 cm^{-1}, a medium-strength ν_4 vibration at 610 cm^{-1}, and a weak ν_1 vibration at 980 cm^{-1}, which are similar to those previously assigned by BIGHAM *et al.* (1990, 1994). Spectral features in the range 445–480 cm^{-1} have been assigned to a ν_2 sulfate mode for hydrated ferric sulfates (ROSS, 1974). Therefore, the absorption feature observed at 465 cm^{-1} in the transmittance spectra of samples Bt-4 and Z510b, is assigned here to a ν_2 symmetric sulfate bending vibration. When the sulfate group exhibits lower than Td symmetry, the ν_2, ν_3, and ν_4 sulfate bending vibrations are often split into multiple vibrations (FARMER, 1974). A strong spectral feature is observed near 1045 and 1070 cm^{-1} in transmittance spectra of samples Bt-4 and Z510b, respectively (Fig. 6, Table 3). A similar feature has been assigned as a degenerate ν_3 vibration in schwertmannite (BIGHAM *et al.,* 1994), but may also be partially due to a ν_2 SO_3 symmetric stretching vibration of acid sulfate species, forming in the schwertmannite tunnels or along the grain surfaces. The ν_1 vibrational feature near 980 cm^{-1} is often not observed in sulfates unless the structure is slightly distorted (ROSS, 1974). This deviation from Td structure is accompanied by the appearance of

a band near 530 cm^{-1} and a shifting of the ν_4 feature near 610 cm^{-1} towards lower wavenumbers. As the ν_2 and ν_4 vibrations are often degenerate for lower symmetry sites, the feature observed near 520 cm^{-1} in the schwertmannite transmittance spectra could be due to either a ν_2 or ν_4 vibration; alternatively, this feature could be due to the presence of acid sulfate groups.

In addition, a weak spectral feature is observed near 1200 cm^{-1} in the reflectance, transmittance and ATR spectra of both samples (Fig. 6), that has been assigned to a degenerate ν_3 vibration in schwertmannite (BIGHAM *et al.* (1994), but would also be consistent with an acid sulfate vibrational mode (ROSS, 1974). Transmittance spectra of schwertmannite mixed with KBr (not shown) exhibited a much stronger absorption near 1200 cm^{-1} indicating that this feature is related to reaction of the sample. KBr reacting with water in the schwertmannite could be protonating some of the sulfate species. Protonation or hydration of the $O—SO_3^-$ ligand is likely if water is present and probably occurs instead of formation of bridging ligands in some cases. BIGHAM *et al.* (1990) pointed out that stretching vibrations occurring at wavenumbers greater than 1200 cm^{-1} indicate the presence of non-bridging sulfate bonds, whereas stretching vibrations occurring at wavenumbers less than 1200 cm^{-1} indicate the presence of sulfates as bidentate bridging complexes (NAKAMOTO, 1986). The non-bridging sulfates would be more likely to form S—OH acid sulfate bonds than the sulfate species acting as bidentate (or doubly) bridging ligands. This is consistent with the spectral feature observed near 1220 cm^{-1} in reflectance spectra (or near 1190 cm^{-1} in transmittance spectra) as resulting from an acid sulfate stretching vibration. The fact that this feature is observed weakly in all spectra indicates that some of the sulfate species in schwertmannite exist in the form of $SO_3(OH)$, as well as SO_4.

Weak spectral features near 1130 and 1030 cm^{-1} were observed in spectra of ferric sulfate-bearing montmorillonites and the intensity of these features was found to increase with the sulfate content of the samples (BISHOP *et al.*, 1995). These are similar to weak features observed in reflectance spectra of schwertmannite and strong features observed in transmittance spectra of schwertmannite.

Recent telescopic observations of Mars have shown a weak feature near 4.5 μm that has been attributed to sulfates in the surface material or atmospheric dust (BLANEY and MCCORD, 1995). Comparison of spectra from 4.4–5.1 μm across several regions of Mars (BLANEY and MCCORD, 1995) shows variations in the spectral slope in the range 4.5–4.8 μm. The reflectance spectra of schwertmannite (Fig. 5a) exhibit a relative reflectance maximum near 4.4 μm and a broad absorption feature from 4.5–5.0 μm. A decrease in reflectance of greater that 10% was observed in our spectra from 4.5–4.8 μm. Perhaps this broad schwertmannite feature is related to the subtle slope changes observed in the martian spectra. Other sulfate minerals, such as jarosite (Fig. 5b), as well as gypsum and anhydrite (BLANEY and MCCORD, 1995), exhibit sharper features in this region. Given mixing of multiple materials in the Mars soil and the large spatial regions observed, the specific sulfate mineral(s) responsible for the spectral observations near 4.5 μm cannot be determined at this time.

Variations in the spectral character of schwertmannites

The trace amounts of goethite and jarosite present in sample Bt-4 (as evidenced by XRD data and weak mid-IR spectral features) do not appear to influence the extended visible region spectral properties as the Bt-4 spectrum is brighter than the Z510b spectrum, whereas the impurities all give darker spectra in this region.

Subtle differences in the character of the extended visible region spectral features between the natural and synthetic schwertmannites (Fig. 2) imply minor structural variations between these two samples. The reflectance maximum in sample Bt-4 occurs at 0.740 μm for both the bulk and <45 μm samples, while it occurs at 0.730 μm for sample Z510b. The $6A_1 \rightarrow 4T_1$ band is broad and nearly flat from 0.900 to 0.915 μm for both samples, although the band minimum lies at 0.915 μm for sample Bt-4 and at 0.918 μm for sample Z510b. Based on colorimetric measurements, samples Bt-4 and Z510b are fairly similar to each other compared to the range of schwertmannites examined so far (*e.g.*, BIGHAM *et al.*, 1992). This is consistent with the similarities in the extended visible region reflectance spectra of samples Bt-4 and Z510b. Optical spectra of other schwertmannites have not yet been measured in this region.

Reflectance spectra of particulate samples have been observed to exhibit brighter near-infrared reflectance and slightly shallower band depths in the visible and near-infrared regions for smaller particle size separates than for larger size separates of the same mineral (*e.g.*, CROWN and PIETERS, 1987). No significant spectral differences were observed in the visible region as a function of particle size

for sample Bt-4. Schwertmannite is generally composed of ultra fine-grained particles that cluster together forming larger aggregates, much like what is observed for smectites. Individual grain sizes of natural and synthetic schwertmannites are on the order of 0.2–0.5 μm (BIGHAM *et al.*, 1994). Therefore, the Bt-4 schwertmannite that was dry sieved in this study to <45 μm particle size may not be very different from the bulk schwertmannite sample. Near-infrared reflectance spectra of the bulk and <45 μm Bt-4 sample, measured under H_2O- and CO_2-purged conditions, showed no significant differences; however, spectra (not shown) of these samples measured under ambient conditions showed increased water absorption in the <45 μm sieved sample.

The reflectance spectra of the two schwertmannite samples measured here are very dark in the surface-scattering region. This is also consistent with small (few μm) grain size. A reflectance minimum or Christiansen feature is observed near 1160 cm^{-1} (~8.6 μm) for both particle size separates of Bt-4 and near 1220 cm^{-1} (~8.2 μm) with a shoulder near 1160 cm^{-1} (~8.6 μm) for sample Z510b. Some subtle variations in band position and shape exist, as well, for several of the mid-IR features shown in Fig. 6 and listed in Table 3. This is consistent with small variations in chemical composition and XRD analyses for several schwertmannites (BIGHAM *et al.*, 1990).

APPLICATIONS FOR MARS

Numerous materials are currently under study as potential analogs for the surface soil on Mars; however, few of these contain substantial amounts of S. The martian soils measured by Viking contained 6.5 to 9.5 wt.% SO_3 (TOULMIN *et al.*, 1977). Because of these large variations in S contents at different sites along the surface (TOULMIN *et al.*, 1977; BAIRD *et al.*, 1977), it is important and interesting to find out what sulfate minerals or salts are present in the martian soil. Perhaps knowing what these sulfate-bearing phases are will provide clues to the chemical weathering processes that occurred on Mars. How much of this fine-grained surface material is present on Mars is not well known, but it may be as deep as several meters in some areas, such as the Tharsis region (CHRISTENSEN and MOORE, 1992).

The extended visible region spectral character of schwertmannite includes a gently sloping shoulder near 0.6 μm, a reflectance maximum at 0.730–0.740 μm, and a broad absorption band having a minimum near 0.915 μm. This is consistent with the spectra of Mars in many regions (*e.g.*, MCCORD *et al.*, 1982; BELL *et al.*, 1990; MURCHIE *et al.*, 1993). The minerals schwertmannite and ferrihydrite often form together (BIGHAM *et al.*, 1992; BIGHAM *et al.*, 1994; SCHWERTMANN *et al.*, 1995); ferrihydrite has been found in at least one meteorite thought to have come from Mars (TREIMAN *et al.*, 1993) and exhibits spectral features similar to those observed for some regions on Mars (BISHOP *et al.*, 1993). BURNS (1994) and BIGHAM *et al.* (1996) have described the geochemical formation patterns of schwertmannite and ferrihydrite under warm and humid conditions, followed by long-term stability under dry conditions. Geochemical and thermodynamic analyses of possible weathering products on Mars indicate that all of the "essential ingredients" for formation of ferric oxyhydroxy sulfate minerals such as schwertmannite existed on Mars (BURNS, 1987, 1988). Although none of these findings are direct evidence for the presence of schwertmannite on Mars, they imply that schwertmannite could be a component of the martian soil.

Ferric sulfate-bearing montmorillonites exhibit similar spectral properties in the extended visible region, except that the broad band minimum occurs at slightly shorter wavelengths (~0.89 μm) than in the spectra of schwertmannite. As this band position in spectra of ferrihydrite, another mineral thought to be present in the ferric sulfate-bearing montmorillonites, is at still longer wavelengths (0.91–0.93 μm), a third ferric component with a shorter wavelength band here must be present as well in the ferric sulfate-bearing montmorillonites. A combination of schwertmannite, ferrihydrite, and smectites is a possible model for the surface material on Mars in the uncommon bright regions, where a longer-wavelength ferric band is observed. A combination of schwertmannite, ferrihydrite, hematite, and smectites is a possible model for the surface material on Mars in the more common bright regions, where the primary ferric absorption occurs near 0.86 μm. Other plausible analogs include terrestrial palagonitic soils and crystalline hematite—nanophase hematite—silicate mixtures. The fine-grained nature of these materials is consistent with the texture observed for the martian surface soil. Schwertmannite, ferrihydrite, and smectites are weathering products that could have formed during an earlier, wetter time on Mars, and would have persisted during the more recent period of aridity.

The concept of a salt-cemented soil, or "duricrust", on Mars was first presented by BINDER *et al.* (1977). Chemical analyses of this martian duricrust showed higher S and Cl abundances, but oth-

erwise little chemical difference from the surface fines (CLARK *et al.,* 1982). Statistical analyses of these elemental trends indicate that sulfates on Mars are correlated with either Mg, Ca, Al or Fe cations (CLARK and VAN HART, 1981). GREELEY *et al.* (1992) suggested that this duricrust is composed of fine-grained particles held together by soluble salts. CLARK *et al.* (1982) interpreted duricrust on Mars as "sulfate salt-enriched and cemented variants of the fines material". The chemically-treated montmorillonites included in this study contain ferric sulfate- and ferric oxide-bearing species that were allowed to form in and around the smectite clay grains in an aqueous environment. Based on the spectral properties of these chemically-treated montmorillonites and other factors, clusters of schwertmannite, ferrihydrite and amorphous ferric iron and sulfate complexes coating the surfaces of smectite grains or aggregates have been proposed as a possible model for duricrust (BISHOP *et al.,* 1995). Were schwertmannite present on Mars, it could act as a binding agent for silicate particles and nanophase ferric oxides, thus resulting in a cemented soil or duricrust having an elevated S content, but otherwise similar chemical composition to the more dust-like surface material on Mars.

Schwertmannite forms under aqueous conditions at low pH in the presence of high concentrations of iron and sulfur and an oxidant (BIGHAM *et al.,* 1992). Schwertmannite often forms together with ferrihydrite, goethite, or jarosite. Which of these minerals form is highly dependent on the concentrations of Fe and S and the pH. SO_4^{2-} concentrations between 1000 and 3000 ppm and pH values between 3 and 4 favor schwertmannite formation (BIGHAM *et al.,* 1992). Future analyses of the martian surface material may provide evidence of schwertmannite or other ferric minerals, and thus provide information on the environmental conditions during the formation of these minerals.

Wind ablation and other physical factors have also acted on the martian surface material. Ferric minerals, such as schwertmannite or hematite, may have formed in mineral deposits, then with time become intermixed with the silicate-bearing phases. Alternatively, nanophase ferric minerals such as ferrihydrite or schwertmannite may have formed along smectite grain surfaces or in the smectite interlayer regions. The presence of silica could inhibit the transformation of schwertmannite to hematite as observed previously for ferrihydrite (CARLSON AND SCHWERTMANN, 1981). Nanophase ferric minerals, such as schwertmannite and ferrihydrite, could be precursors to hematite formed during thermal weathering. If localities on Mars are identified where the relative abundance of the nanophase minerals schwertmannite or ferrihydrite vs. the relative abundance of crystalline hematite are different, then those areas having reduced amounts of crystalline hematite could be more sheltered from the processes that produce hematite. Examination of the physical properties of the matrix materials (*i.e.* silicate phase) could lead to insights, as well, into the geochemical conditions during formation and the subsequent weathering of the martian soil.

Given the possibility of schwertmannite on Mars, a pertinent question is: how can it be detected there? The optical spectra of schwertmannite are distinct from those of many other iron oxides and sulfates; however, high spatial-resolution and high spectral-resolution spectra would be required to differentiate schwertmannite from all other ferric minerals. The dominant features in infrared reflectance spectra of schwertmannite are due to OH and H_2O, and are found in the spectra of other hydroxylated minerals such as ferrihydrite. Transmittance spectra of schwertmannite exhibit several strong sulfate and Fe—OH absorption features that are observed only weakly in reflectance spectra. Because of the fine-grained nature of schwertmannite, it is likely that these features would also be weak in emittance spectra. Therefore, high spectral-resolution spectroscopic observation of Mars might provide spectra consistent with that of schwertmannite, but uniquely identifying schwertmannite from visible and infrared spectra alone would be difficult.

KNUDSEN *et al.* (1991) and AGRESTI *et al.* (1992) have designed Mössbauer experiments for Mars that should be useful for characterizing the iron-rich phases on that planet. Because of the asymmetry of its Mössbauer spectra, and because the magnetic hyperfine field of schwertmannite at 4.2 K is lower than that of any iron oxide and jarosite, Mössbauer spectra taken at 4.2 K would be suitable for the identification of this mineral, and its quantification in assemblages of complex iron mineralogy (MURAD *et al.,* 1994). Mössbauer spectra taken in the paramagnetic state are also unique and would allow the identification of schwertmannite in monomineralic samples. The Mössbauer spectra of paramagnetic schwertmannite, however, are not distinctive enough to discern the presence of this mineral in complex mineral mixtures containing substantial amounts of other paramagnetic ferric components.

The best procedure for detecting schwertman-

nite, as in the case of other minerals, would be to combine the results of as many techniques as possible. Optical, infrared and Mössbauer spectroscopy, X-ray fluorescence, and X-ray diffraction would be useful. A sample return mission might facilitate a number of these analyses; however, as mentioned by KNUDSEN *et al.* (1991), it is possible that the oxidation state of the iron component might be altered during transit. For this reason, *in situ* measurements of the martian surface materials would be advantageous.

CONCLUSIONS

The reflectance spectrum of schwertmannite is dominated by a broad ferric band near 0.91 μm and a broad water band near 3 μm. These features are consistent with spectra of some areas on Mars. The optical and Mössbauer spectra show evidence of the ferric sites in the schwertmannite structure, namely Fe(III) octahedrally coordinated as $FeO_3(OH)_3$ and $FeO_3(OH)_2O—SO_3$. The extended visible region reflectance spectra of natural and synthetic schwertmannite are characterized by a steep incline near 0.5 μm, a gently sloping shoulder near 0.6 μm, a reflectance maximum at 0.73–74 μm, and a broad band with a minimum at 0.915–0.918 μm. Additional infrared spectral features due to bound and adsorbed water are observed at 1.45, 1.95, and 6.1 μm. Numerous spectral features from ~8–25 μm (~1200–400 cm^{-1}) are due to sulfate and OH species.

The results of optical, infrared, and Mössbauer spectroscopy indicate that ferric sulfate-bearing montmorillonites, prepared as Mars soil analog materials, contain schwertmannite or a schwertmannite-like phase. Schwertmannite could be present in the surface material on Mars, intermixed with other ferric minerals, such as ferrihydrite, and with silicates, such as smectites. High-resolution visible to infrared spectroscopy and low-temperature Mössbauer spectroscopy of the martian soil would be useful for detection of schwertmannite if it is present on Mars. Identifying the ferric oxide minerals and silicate components of the martian soil would provide information about the chemical weathering processes on Mars.

Acknowledgements—We are indebted to U. SCHWERTMANN for placing schwertmannite samples at our disposal and providing access to room-temperature Mössbauer facilities and to F. E. WAGNER for providing access to liquid-helium Mössbauer facilities. We would like to express gratitude to A. DUMMEL, T. HIROI and S. PRATT for technical assistance and to J. F. BELL, V. C. FARMER, R. V. MORRIS, S. MURCHIE, and U. SCHWERTMANN for helpful editorial comments. Financial support from the Alexander von Humboldt Foundation and use of the facilities at the DLR-Berlin are much appreciated by J. BISHOP. The RELAB and Nicolet spectrometers at Brown University are part of a multi-user system supported by NASA grant NAGW-748.

REFERENCES

ADAMS J. and MCCORD T. B. (1969) Mars: Interpretation of spectral reflectivity of light and dark regions. *J. Geophys. Res.* **74**, 4851–4856.

AFANASEV A. M., GOROBCHENKO V. D., KULGAWCZUK D. S. and LUKASHEVICH I. I. (1974) Nuclear γ-resonance in iron sulphates of the jarosite group. *Phys. Stat. Sol.(a)* **26**, 697–701.

AGRESTI D. G., MORRIS R. V., WILLS E. L., SHELFER T. D., PIMPERL M. M., SHEN M.-H., CLARK B. C. and RAMSEY B. D. (1992) Extraterrestrial Mössbauer spectrometry. *Hyperfine Interactions* **72**, 285–298.

ARNOLD G. (1992) Infrarotsondierung planetarer Oberflächen. *Dtsch. Luft Raumfahrt-Nachrichten* **69**, 25–31.

BAIRD A. K., CASTRO A. J., CLARK B. C. III, TOULMIN P. III, ROSE H. J. JR., KEIL K. and GOODING J. L. (1977) The Viking X ray fluorescence experiment: Sampling strategies and laboratory simulations. *J. Geophys. Res.* **82**, 4595–4624.

BANIN A. and RISHPON J. (1979) Smectite clays in Mars soil: Evidence for their presence and role in viking biology experimental results. *J. Molecular Evolution* **14**, 133–52.

BANIN A., CARLE G., CHANG S., COYNE L., ORENBERG J. and SCATTERGOOD T. (1988) Laboratory investigations of Mars: Chemical and spectroscopic characteristics of a suite of clays as Mars soil analogs. *Origins of Life and Evolution of the Biosphere* **18**, 239–265.

BANIN A., CLARK B. C. and WÄNKE H. (1992) Surface chemistry and mineralogy. In *Mars* (eds. H. KIEFFER *et al.*), pp. 594–625. Univ. Arizona Press, Tucson.

BANIN A., BEN-SHLOMO T., MARGULIES L., BLAKE D. F., MANCINELLI R. L. and GEHRING A. U. (1993) The nanophase iron minerals in Mars soil. *J. Geophys. Res.* **98**, 20831–20853.

BEINROTH A. and ARNOLD G. (1996) Analysis of weak surface absorption bands in the ISM (Phobos-2) near-infrared spectra of Mars. *Vibrational Spectroscopy,* in press. **11,** in press.

BELL J. F. III (1992) Charge-coupled device imaging spectroscopy of Mars. 2. Results and implications for martian ferric mineralogy. *Icarus* **100,** 575–597.

BELL J. F. III and CRISP D. (1993) Groundbased imaging spectroscopy of Mars in the near-infrared: Preliminary results. *Icarus* **104,** 2–19.

BELL J. F. III, MCCORD T. B. and OWENSBY P.D. (1990) Observational evidence of crystalline iron oxides on Mars. *J. Geophys. Res.* **95,** 14447–14461.

BELL J. F. III, POLLACK J. B., GEBALLE T. R., CRUIKSHANK D. P. and FREEDMAN R. (1994) Spectroscopy of Mars from 2.04 to 2.44 μm during the 1993 opposition: Absolute calibration and atmospheric vs mineralogic

origin of narrow absorption features. *Icarus* **111,** 106–123.

BIBRING J.-P., COMBES M., LANGEVIN Y., CARA C., DROSSART P., ENCRENAZ T., ERARD S., FORNI O., GONDET B., KSANFOMALITI L., LELLOUCH E., MASSON P., MOROZ V., ROCARD F., ROSENQVIST J., SOTIN C. and SOUFFLOT A. (1990) ISM observations of Mars and Phobos: First results. *Proceedings 20th Lunar Planet. Science Conf.,* LPI, Houston, pp. 461–471.

BIGHAM J. M., SCHWERTMANN U., CARLSON L. and MURAD E. (1990) A poorly crystallized oxyhydroxysulfate of iron formed by bacterial oxidation of Fe(II) in acid mine waters. *Geochim. Cosmochim. Acta* **54,** 2743–2758.

BIGHAM J. M., SCHWERTMANN U. and CARLSON L. (1992) Mineralogy of precipitates formed by the biogeochemical oxidation of Fe(II) in mine drainage. In *Biomineralization Processes of Iron and Manganese—Modern and Ancient Environments* (eds. H. C. W. SKINNER and R. W. FITZPATRICK), pp. 219–232, Catena Verlag.

BIGHAM J. M., CARLSON L. and MURAD E. (1994) Schwertmannite, a new iron oxyhydroxysulfate from Pyhäsalmi, Finland, and other localities. *Miner. Mag.* **58,** 641–648.

BIGHAM J. M., SCHWERTMANN U., TRAINA S. J., WINLAND R. L. and WOLF M. (1996) Schwertmannite and the chemical modeling of iron in acid sulfate waters. *Geochim. Cosmochim. Acta* **60,** 2111–2121.

BINDER A. B., ARVIDSON R. E., GUINNESS E. A., JONES K. L., MORRIS E. C., MUTCH T. A., PIERI D. C. and SAGAN C. (1977). The geology of the Viking Lander 1 site. *J. Geophys. Res.* **82,** 4439–4451.

BISHOP J. L. and PIETERS C. M. (1995) Low-temperature and low atmospheric pressure infrared reflectance spectroscopy of Mars soil analog materials. *J. Geophys. Res.* **100,** 5369–5379.

BISHOP J. L., PIETERS C. M. and BURNS R. G. (1993) Reflectance and Mössbauer spectroscopy of ferrihydrite-montmorillonite assemblages as Mars soil analog materials. *Geochim. Cosmochim. Acta* **57,** 4583–4595.

BISHOP J. L., PIETERS C. M. and EDWARDS J. O. (1994) Spectroscopic analyses on the nature of water in montmorillonite. *Clays Clay Minerals* **42,** 702–716.

BISHOP J. L., PIETERS C. M., BURNS R. G., EDWARDS J. O., MANCINELLI R. L. and FRÖSCHL H. (1995) Reflectance spectroscopy of ferric sulfate-bearing montmorillonites as Mars soil analog materials. *Icarus* **117,** 101–119.

BLANEY D. L. and MCCORD T. B. (1989) An observational search for carbonates on Mars. *J. Geophys. Res.* **94,** 10159–10166.

BLANEY D. L. and MCCORD T. B. (1995) Indications of sulfate minerals in the martian soil from Earth-based spectroscopy. *J. Geophys. Res.* **100,** 14433–14441.

BRADY K. S., BIGHAM J. M., JAYNES W. F. and LOGAN T. J. (1986) Influence of sulfate on Fe-oxide formation: Comparisons with a stream receiving acid mine drainage. *Clays Clay Miner.* **34,** 226–274

BURNS R. G. (1987) Ferric sulfates on Mars. *Proc. 17th Lunar Planet. Sci. Conf.* LPI, Houston, E570–574.

BURNS R. G. (1988) Gossans on Mars. *Proc. 18th Lunar Planet. Sci. Conf.* LPI, Houston, 713–721.

BURNS R. G. (1993a) Rates and mechanism of chemical weathering of ferromagnesian silicate minerals on Mars. *Geochim. Cosmochim. Acta* **57,** 4555–4574.

BURNS R. G. (1993b) *Mineralogical Applications of Crystal Field Theory.* 2nd Ed. Cambridge Univ. Press.

BURNS R. G. (1994) Schwertmannite on Mars: Deposition of this ferric oxyhydroxysulfate mineral in acidic saline meltwaters (abstr.). *Lunar and Planet. Sci.* **XXV,** 203–204.

BURNS R. G. and FISHER D. S. (1993) Rates of oxidative weathering on the surface of Mars. *J. Geophys. Res.* **98,** 3365–3372.

CARLSON L. and SCHWERTMANN U. (1981) Natural ferrihydrites in surface deposits from Finland and their association with silica. *Geochim. Cosmochim. Acta* **45,** 421–429.

CARR M. H. (1981) *The Surface of Mars.* Yale Univ. Press, New Haven.

CARR M. H. (1995) The martian drainage system and the origin of valley networks and fretted channels. *J. Geophys. Res.* **100,** 7479–7507.

CHRISTENSEN P. R. and MOORE H. J. (1992) The martian surface layer. In *Mars* (eds. H. KIEFFER *et al.*), pp 686–729. Univ. Arizona Press, Tucson.

CLARK B. C. (1993) Geochemical components in martian soil. *Geochim. Cosmochim. Acta* **57,** 4575–4581.

CLARK B. C. and VAN HART D. C. (1981) The salts of Mars. *Icarus* **45,** 370–378.

CLARK B. C. III, BAIRD A. K., ROSE H. J. JR., TOULMIN P. III, CHRISTIAN R. P., KELLIHER W. C., CASTRO A. J., ROWE C. D., KEIL K. and HUSS G. R. (1977) The Viking X ray fluorescence experiment: Analytical methods and early results. *J. Geophys. Res.* **82,** 4577–4594.

CLARK B. C., BAIRD A. K., WELDON R. J., TSUSAKI D. M., SCHNABEL L. and CANDELARIA M. P. (1982) Chemical composition of martian fines. *J. Geophys. Res.* **87,** 10059–10067.

CLARK R. N. and ROUSH T. L. (1984) Reflectance spectroscopy: Quantitative analysis techniques for remote sensing applications. *J. Geophys. Res.* **89,** 6329–6340.

CLARK R. N., SWAYZE G. A., SINGER R. B. and POLLACK J. B. (1990) High-resolution reflectance spectra of Mars in the 2.3 μm region: Evidence for the mineral scapolite. *J. Geophys. Res.* **95,** 14463–14480.

CONEL J. E. (1969) Infrared emissivities of silicates: Experimental results and a cloudy atmosphere model of spectral emission from condensed particulate mediums. *J. Geophys. Res.* **74,** 1614–1634.

CROWN D. A. and PIETERS C. M. (1987) Spectral properties of plagioclase and pyroxene mixtures and the interpretation of Lunar soil spectra. *Icarus* **72,** 492–506.

ERARD S., BIBRING J.-P., MUSTARD J., FORNI O., HEAD J. W., HURTREZ S., LANGEVIN Y., PIETERS C. M., ROSENQVIST J. and SOTIN C. (1991) Spatial variations in composition of the Valles Marineris and Isidis Planitia regions of Mars derived from ISM data. *Proc. 21st Lunar Planet. Sci. Conf.,* LPI, Houston, 437–455.

FANALE F. P., POSTAWKO S. E., POLLACK J. B., CARR M. H. and PEPIN R. O. (1992) Mars: Epochal climate change and volatile history. In *Mars* (eds. H. KIEFFER *et al.*), pp. 1135–1179. Univ. Arizona Press, Tucson.

FARMER J. (1995) Did Mars once harbor life? *EOS* **76,** 442.

FARMER V. C. (1974) The layer silicates. In *The Infrared Spectra of Minerals* (ed. V. C. FARMER), pp. 331–363. Bartholomew Press.

GAFFEY S. J., MCFADDEN L. A., NASH D. and PIETERS C. M. (1993) Ultraviolet, visible, and near-infrared reflectance spectrsocopy: Laboratory spectra of geologic materials. In *Remote Geochemical Analyses: Elemental and Mineralogical Composition* (eds. C. M. PIETERS and P. ENGLERT), pp. 367–393. Cambridge Univ. Press.

GOLDEN D. C., MORRIS R. V., MING D. W., LAUER H. V. JR. and YANG S. R. (1993) Mineralogy of three slightly palagonitized basaltic tephra samples from the summit of Mauna Kea, Hawaii. *J. Geophys Res.* **98,** 3401–3411.

GOODING J. L. (1978) Chemical weathering on Mars. *Icarus* **33,** 483–513.

GOODING J. L. and KEIL K. (1978) Alteration of glass as a possible source of clay minerals on Mars. *Geophys. Res. Let.* **5,** 727–730.

GOODING J. L., ARVIDSON R.E. and ZOLOTOV M. Y. (1992) Physical and chemical weathering. In *Mars* (eds. H. KIEFFER *et al.*), pp. 626–651. Univ. Arizona Press, Tucson.

GREELEY R., LANCASTER N., LEE S. and THOMAS P. (1992) Martian aeolian processes, sediments, and features. In *Mars* (eds. H. KIEFFER *et al.*), pp.730–766. Univ. Arizona Press, Tucson.

HANEL R. B., CONRATH B., HOVIS W., KUNDE V., LOWMAN P., MAGUIRE W., PEARL J., PIRRAGLIA J., PRABHAKARA C. and SCHLACHMAN B. (1972) Investigation of the martian environment by infrared spectroscopy on Mariner 9. *Icarus* **17,** 423–442.

HOUCK J. R., POLLACK J. B., SAGAN C., SCHAACK D. and DECKER J. A. JR. (1973) High altitude infrared spectroscopic evidence for bound water on Mars. *Icarus* **18,** 470–480.

HUHEEY J. E., KEITER E. A. and KEITER R. L. (1993) *Inorganic Chemistry.* 4th Ed. HarperCollins, New York.

HUNT G. R., LOGAN L. M. and SALISBURY J. W. (1973) Mars: Components of infrared spectra and the composition of the dust cloud. *Icarus* **18,** 459–469.

JAKOSKY B. M. and HABERLE R. M. (1992) The seasonal behavior of water on Mars. in *Mars*, eds. H. KIEFFER *et al.*, Univ. Arizona Press, Tucson, 969–1016.

KIEFFER H. H., MARTIN T. Z., PETERFREUND A. R., JAKOSKY B. M., MINER E. D. and PALLUCONI F. D. (1977) Thermal and albedo mapping of Mars during the Viking primary mission. *J. Geophys. Res.* **82,** 4249–4291.

KNUDSEN J. M., MADSEN M. B., OLSEN M., VISTISEN L., KOCH C. B., MØRUP S., KANKELEIT E., KLINGELHÖFER G., EVLANOV E. N., KHROMOV V. N., MUKHIN L. M., PRILUTSKI O. F., ZUBKOV B., SMIRNOV G. V. and JUCHNIEWICZ J. (1991) Mössbauer spectroscopy on the surface of Mars. Why? *Hyperfine Interact.* **68,** 83–94.

MCCORD T. B., HUGUENIN R. L., MINK D. and PIETERS C. (1977) Spectral reflectance of martian areas during the 1973 opposition: Photoelectric filter photometry. *Icarus* **31,** 25–39.

MCCORD T. B., CLARK R. N. and HUGUENIN R. L. (1978) Mars: Near-infrared spectral reflectance and compositional implications. *J. Geophys. Res.* **83,** 5433–5441.

MCCORD T. B., CLARK R. N. and SINGER R. B. (1982) Mars: Near-infrared spectral reflectance of surface regions and compositional implications. *J. Geophys. Res.* **87,** 3021–3032.

MORRIS R. V. and LAUER H. V. JR. (1990) Matrix effects for reflectivity spectra of dispersed nanophase (superparamagnetic) hematite with application to martian spectral data. *J. Geophys Res.* **95,** 5101–5109.

MORRIS R. V., LAUER H. V. JR., LAWSON C. A., GIBSON E. K. JR., NACE G. A. and STEWART C. (1985) Spectral and other physicochemical properties of submicron powders of hematite (α-Fe_2O_3), maghemite (γ-Fe_2O_3), magnetite (Fe_3O_4), goethite (α-FeOOH), and lepidocrocite (γ-FeOOH). *J. Geophys. Res.* **90,** 3126–3144.

MORRIS R. V., AGRESTI D. G., LAUER H. V. JR., NEWCOMB J. A., SHELFER T. D. and MURALI A. V. (1989) Evidence for pigmentary hematite on Mars based on optical, magnetic and Mössbauer studies of superparamagnetic (nanocrystalline) hematite. *J. Geophys Res.* **94,** 2760–2778.

MORRIS R. V., GOODING J. L., LAUER H. V. JR. and SINGER R. B. (1990) Origins of marslike spectral and magnetic properties of a Hawaiian palagonitic soil. *J. Geophys Res.* **95,** 14427–14434.

MORRIS R. V., SCHULZE D. G., LAUER H. V. JR., AGRESTI D. G. and SHELFER T. D. (1992) Reflectivity (visible and near IR), Mössbauer, static magnetic, and X ray diffraction properties of aluminum-substituted hematites. *J. Geophys Res.* **97,** 10257–10266

MORRIS R. V., GOLDEN D. C., BELL J. F., LAUER H. V. and ADAMS J. B. (1993) Pigmenting agents in martian soils: Inferences from spectral, Mössbauer, and magnetic properties of nanophase and other iron oxides in Hawaiian palagonitic soil PN-9. *Geochim. Cosmochim. Acta* **57,** 4597–4609.

MURAD E. (1988) The Mössbauer spectrum of "well"-crystallized ferrihydrite. *J. Magnetism Magnetic Mater.* **74,** 153–157.

MURAD E. (1996) Magnetic properties of microcrystalline iron(III) oxides and related materials as reflected in their Mössbauer spectra. *Phys. Chem. Miner.* **23,** in press.

MURAD E. and JOHNSTON J. H. (1987) Iron oxides and oxyhydroxides. In *Mössbauer Spectroscopy Applied to Inorganic Chemistry* (ed. G. J. Long), Vol.2, pp. 507–582. Plenum Pub.

MURAD E., BIGHAM J. M., BOWEN L. H. and SCHWERTMANN U. (1990) Magnetic properties of iron oxides produced by bacterial oxidation of Fe^{2+} under acid conditions. *Hyperfine Interact.* **58,** 2373–2376.

MURAD E., SCHWERTMANN U., BIGHAM J. M. and CARLSON L. (1994) The mineralogical characteristics of poorly crystalline precipitates formed by oxidation of Fe^{2+} in acid sulfate waters. In *Environmental Geochemistry of Sulfide Oxidation* (eds. C. N. ALPERS and D. W. BLOWES), pp. 191–200, American Chemical Society.

MURCHIE S., MUSTARD J., BISHOP J., HEAD J. and PIETERS C. (1993) Spatial variations in the spectral properties of bright regions on Mars. *Icarus* **105,** 454–468.

NAKAMOTO K. (1986) *Infrared and Raman Spectra of Inorganic and Coordination Compounds,* 4th ed. J. Wiley & Sons.

ORENBERG J. and HANDY J. (1992) Reflectance spectroscopy of palagonite and iron-rich montmorillonite clay mixtures: Implications for the surface composition of Mars. *Icarus* **96,** 219–225.

PIETERS C. M. (1983) Strength of mineral absorption features in the transmitted component of near-infrared reflected light: First results from RELAB. *J. Geophys Res.* **88,** 9534–9544.

PIMENTEL G. C., FORNEY P. B. and HERR K. C. (1974) Evidence about hydrate and solid water in the martian surface from the 1969 Mariner infrared spectrometer. *J. Geophys. Res.* **79,** 1623–1634.

POLLACK J. B., KASTING J. F., RICHARDSON S. M. and POLIAKOFF K. (1987) The case for a warm, wet climate on early Mars. *Icarus* **71,** 203–224.

POLLACK J. B., ROUSH T., WITTEBORN F., BREGMAN J., WOODEN D., STOKER C., TOON O., RANK D., DALTON B. and FREEDMAN R. (1990) Thermal emission spectra

of Mars (5.4–10.5 μm): Evidence for sulfates, carbonates, and hydrates. *J. Geophys. Res.* **95,** 14595–14627.

Ross S. D. (1974) Sulphates and other oxy-anions of Group VI. In *The Infrared Spectra of Minerals* (ed. V. C. Farmer), pp. 423–444. Bartholomew Press.

Roush T. L., Blaney D. L. and Singer R. B. (1993) The surface composition of Mars as inferred from spectroscopic observations. In *Remote Geochemical Analyses: Elemental and Mineralogical Composition* (eds. C. M. Pieters and P. Englert), pp. 367–393. Cambridge Univ. Press.

Salisbury J. W. (1993) Mid-infrared spectroscopy: Laboratory data. In *Remote Geochemical Analyses: Elemental and Mineralogical Composition* (eds. C. M. Pieters and P. Englert), pp. 367–393. Cambridge Univ. Press.

Salisbury J. W., Walter L. S., Vergo N. and D'Aria D. M. (1991) *Infrared (2.1–25 μm) Spectra of Minerals,* Johns Hopkins Univ. Press.

Schwertmann U. and Cornell R. M. (1991) *Iron Oxides in the Laboratory,* VCH Publishers.

Schwertmann U., Bigham J. and Murad E. (1995) The first occurrence of schwertmannite in a natural stream environment. *Eur. J. Miner.* **7,** 547–552.

Sherman D. M. and Waite T. D. (1985) Electronic spectra of Fe^{3+} oxides and oxide hydroxides in the near-IR to near-UV. *Amer. Miner.* **70,** 1262–1269.

Sherman D. M., Burns R. G. and Burns V. M. (1982) Spectral characterization of the iron oxides with application to the martian bright region mineralogy. *J. Geophys Res.* **87,** 10,169–10,180.

Singer R. B. (1982) Spectral evidence for the mineralogy of high-albedo soils and dust on Mars. *J. Geophys. Res.* **87,** 10,159–10,168.

Singer R. B., McCord T. B., Clark R. N., Adams J. B. and Huguenin R. L. (1979) Mars surface composition from reflectance spectroscopy: A summary. *J. Geophys. Res.* **84,** 8415–8426.

Soderblom L. A. (1992) The composition and mineralogy of the martian surface from spectroscopic observations: 0.3 μm to 50 μm. In *Mars* (eds. H. Kieffer *et al.*), pp. 557–593. Univ. Arizona Press, Tucson.

Toulmin P. III, Baird A. K., Clark B. C., Keil K., Rose H. J. Jr., Christian R. P., Evans P. H. and Kelliher W. C. (1977) Geochemical and mineralogical interpretation of the Viking inorganic chemical results. *J. Geophys. Res.* **82,** 4625–4634.

Treiman A. H., Barrett R. A. and Gooding J. L. (1993) Preterrestrial aqueous alteration of the Lafayette (SNC) meteorite. *Meteoritics* **28,** 86–97.